Predictive regulatory and metabolic network models for systems analysis of *Clostridioides difficile*

Mario L. Arrieta-Ortiz[1], Selva Rupa Christinal Immanuel[1], Serdar Turkarslan[1], Wei Ju Wu[1], Brintha P. Girinathan[2], Jay N. Worley[2], Nicholas DiBenedetto[2], Olga Soutourina[3], Johann Peltier[3], Bruno Dupuy[4], Lynn Bry[2] and Nitin S. Baliga[1,+]

1. Institute for Systems Biology, Seattle, WA, USA
2. Massachusetts Host-Microbiome Center, Dept. Pathology, Brigham & Women's Hospital, Harvard Medical School, Boston, MA , USA
3. Université Paris-Saclay, CEA, CNRS, Institute for Integrative Biology of the Cell (I2BC), 91198, Gif-sur-Yvette, France
4. Laboratory of the Pathogenesis of Bacterial Anaerobes, Institut Pasteur, Université de Paris, UMR-CNRS2001, France

+corresponding author: nitin.baliga@isbscience.org

ABSTRACT

Though *Clostridioides difficile* is among the most studied anaerobes, we know little about the systems level interplay of metabolism and regulation that underlies its ability to negotiate complex immune and commensal interactions while colonizing the human gut. We have compiled publicly available resources, generated through decades of work by the research community, into two models and a portal to support comprehensive systems analysis of *C. difficile*. First, by compiling a compendium of 148 transcriptomes from 11 studies we have generated an **E**nvironment and **G**ene **R**egulatory **I**nfluence **N**etwork (EGRIN) model that organizes 90% of all genes in the *C. difficile* genome into 297 high quality modules based on evidence for their conditional co-regulation by at least 120 transcription factors. EGRIN predictions, validated with independently-generated datasets, have recapitulated previously characterized *C. difficile* regulons of key transcriptional regulators, refined and extended membership of genes within regulons, and implicated new genes for sporulation, carbohydrate transport and metabolism. Findings further predict pathogen behaviors in *in vivo* colonization, and interactions with beneficial and detrimental commensals. Second, by advancing a constraints-based metabolic model, we have discovered that 15 amino acids, diverse carbohydrates, and 24 genes across glyoxylate, Wood-Ljungdahl, nucleotide, amino acid, and carbohydrate metabolism are essential to support growth of *C. difficile* within an intestinal environment. Models and supporting resources are accessible through an interactive web portal (http://networks.systemsbiology.net/cdiff-portal/) to support collaborative systems analyses of *C. difficile*.

40 # INTRODUCTION

41 *Clostridioides difficile*, the etiology of pseudomembranous colitis, causes more than 500,000
42 infections, 30,000 deaths, and $5 billion per year in US healthcare costs (1). Infections arise
43 through a variety of conditions that modulate the pathogen's ability to colonize and expand in the
44 gut. Antibiotic ablation of the commensal microbiota creates altered nutrient states in intestinal
45 environments due to lack of competition for nutrients from host, dietary or microbial origin. The
46 pathogen modifies its endogenous metabolism to respond to these altered states, which
47 stimulates subsequent cellular programs that can promote enhanced colonization and growth.
48 Stress and starvation responses within *C. difficile* populations trigger responses that lead to
49 sporulation, biofilm formation and release of mucosal damaging toxins (2–4).

50 Symptomatic infection requires the production of toxins from the *C. difficile* pathogenicity locus
51 (PaLoc), which includes the genes *tcdA, tcdB* and *tcdE* that respectively encode the A and B
52 toxins and holin involved in toxin export. The PaLoc also contains *tcdR*, a sigma factor specific
53 for the toxin gene promoters, and *tcdC*, a TcdR anti-sigma factor (5, 6). Epidemic ribotype 027
54 strains carry a second toxin locus, *cdt,* which includes the binary toxin genes *ctdA* and *ctdB*, and
55 *cdtR* regulator, which has also been hypothesized to modulate PaLoc expression (7, 8). *C. difficile*
56 elaborates toxin under starvation conditions to extract nutrients from the host and promote spore
57 shedding (9–11). Regulation of PaLoc expression occurs via a complex network of TFs and small
58 molecule inputs, of which direct primary regulators have been well described, but more complex
59 and combinatorial effects remain unclear (11). Toxin production further triggers rapid and
60 profound host immune responses, including release of reactive oxygen species (ROS) which
61 substantially alters the redox state of the gut environment, and other innate immune responses
62 that can induce *C. difficile* stress responses to cell wall, oxidative, and other damaging stimuli
63 (12–15). As per all microbes, *C. difficile* adapts to complex, dynamic environments through

64 changes in metabolism coordinated by a gene regulatory network (16, 17). However, the
65 mechanisms by which the gene regulatory network and metabolic pathways integrate to modulate
66 *C. difficile* pathogenesis remain ill-defined (18, 19).

67 The *C. difficile* 630 (CD630) genome encodes 4,018 genes, with ~309 putative transcription
68 factors (TFs; including sigma factors), 1,030 metabolic genes, and 1,330 genes (>30%) with
69 unknown function (20, 21). The ATCC43255 strain of *C. difficile,* which is used to generate
70 symptomatic infections in mice, encodes 4,117 genes and ~327 TFs, of which ~97% are
71 significantly orthologous to genes encoded in the CD630 strain (22). To address questions
72 regarding the broader systems-level interplay among genes in colonization and infection, we used
73 computational modeling and network inference algorithms to construct an Environment and Gene
74 Regulatory Influence Network (EGRIN) model for *C. difficile.* This model leverages a compendium
75 of 148 published transcriptomes that surveyed responses of CD630 in diverse contexts. The
76 EGRIN model consists of modules of putatively co-regulated genes identified based on their co-
77 expression over subsets of conditions, enrichment of functional associations, chromosomal
78 proximity, co-occurrence across phylogenetically related organisms, and presence of conserved
79 DNA motif(s) within their promoter regions indicating regulation by the same TFs. Further, using
80 regression analysis, EGRIN also captures the combinatorial regulation of genes within each
81 module as a function of the weighted influences of TFs. The model supports a systems-level
82 understanding of the infective capacity of this obligate anaerobe under different *in vitro* and *in vivo*
83 conditions.

84 In addition to EGRIN, we have advanced a metabolic network model of *C. difficile* to understand
85 how conditional regulation manifests physiologically, by adding reactions and associated genes
86 supporting the exchange of nutrients required for growth in intestinal environments. We apply the
87 EGRIN and metabolic models to predict conditional contributions of metabolic genes to the
88 pathogen's fitness under different environmental conditions. Analyses support rational prediction

89 of context-specific vulnerabilities of the pathogen and uncover TFs driving essential adaptive
90 responses under *in vitro* versus *in vivo* conditions. This analytic framework provides a new
91 systems-level view of the transcriptional and metabolic networks that coordinate *C. difficile's*
92 colonization, growth, expression of toxin, and adaptions to changing environments with host
93 infection. Our models identified multiple TFs that coordinate critical aspects within each of these
94 components, including contributions from PrdR, which regulates the Stickland proline and glycine
95 reductase systems and other energy-generating pathways, and Rex a regulator modulating
96 energy balance in *C. difficile* (23, 24). These findings refine the context and roles of these and
97 other regulators in *C. difficile* virulence, and provide specific targets of vulnerability for model-
98 informed interventions against this pathogen. The compiled datasets, algorithms, and models can
99 be explored interactively through a community-wide web resource at
100 http://networks.systemsbiology.net/cdiff-portal/.

101

102

103

104 # RESULTS

105 **Reconstruction of the environment and gene regulatory influence network (EGRIN) model**
106 **for *C. difficile* 630**

107 To investigate *C. difficile's* transcriptionally-driven adaptive strategies we compiled 148 publicly
108 available transcriptomic datasets from 11 independent studies using CD630 (**Table 1**). This
109 compendium captures diverse transcriptional responses of *C. difficile* to commensals, *in vitro* or
110 *in vivo* responses to different nutrient conditions, and consequences of targeted TF gene
111 deletions. The transcriptome compendium together with functional associations from STRING
112 (25), and all promoter sequences, was analyzed with a suite of network inference tools to infer an
113 EGRIN model for *C. difficile* (**Fig. 1A**). The cMonkey2 biclustering algorithm (26) iteratively
114 grouped functionally-associated genes into **modules** based on their co-expression across
115 subsets of environments, and presence of similar cis-acting gene regulatory elements (**GREs**),
116 providing mechanistic evidence for co-regulation. Subsequently, we used the Inferelator (27) to
117 discover potential TFs of each module through a regression-based approach. The resulting
118 EGRIN model organized 3,895 of 4,018 CD630 genes into 406 gene modules, and inferred
119 module regulation by 148 of 309 genomically identified TFs that putatively act through GREs
120 discovered within gene and operon promoters. Among the Inferelator implicated regulatory
121 networks, 221 modules were controlled by more than one TF, and 75 were regulated by more
122 than two TFs (**Fig. S1**). The TF module assignments support subsequent hypothesis-driven
123 experimental analyses, including the design of ChIP-seq and TF-deletion experiments to validate
124 the regulatory network architecture under physiologically relevant environmental contexts.

125

126 The quality of modules within the EGRIN model was evaluated using residual scores, which reflect
127 the coherence of gene co-expression patterns. The lower the residual score, the higher the quality
128 of the module. We determined using an empirical approach that a residual cutoff of 0.55 identified

129 a functionally meaningful set of 297 high quality modules (73% of the total 406 modules) based
130 on the relative enrichment of related functions within modules that passed filtering (**Fig. 1B**).
131 Incidentally, this empirically determined threshold was similar to the threshold used to identify
132 high quality EGRIN gene modules for *Mycobacterium tuberculosis* (28). Altogether, the 297 high
133 quality modules captured transcriptional regulation of 3,617 genes (90%) in CD630, with average
134 membership of 20 genes per module (**Fig. 1C-D**). These metrics were consistent with models
135 developed for other organisms (28, 29), a remarkable finding given that the transcriptional dataset
136 used to construct the *C. difficile* model was less than 10% the size of ones used to construct
137 models for other species.
138
139 **Validation of the modular architecture and regulatory mechanisms uncovered by the *C.***
140 ***difficile* EGRIN model**
141 We tested the accuracy of the EGRIN model to reconstruct previously characterized regulons and
142 recapitulate key aspects of *C. difficile* biology. To do so, we performed gene enrichment analysis
143 within modules using an updated annotation of *C. difficile* genome (22). This analysis identified
144 93 of 297 modules (31%) with significant enrichment of genes with related functions in 40
145 pathways (hypergeometric test adjusted p-value ≤ 0.05). Among these pathways, 13 were over-
146 represented in three or more modules (**Fig. 2A**), demonstrating the capacity of the model to
147 discover conditional partition of cellular processes. We also investigated whether the EGRIN
148 model had identified known regulatory interactions between TFs and their target genes. We
149 compiled from literature the regulons (i.e. target genes) of 13 previously characterized TFs in *C.*
150 *difficile*, representing a network of 1,353 TF-gene interactions (**Table S1**). Notably, a total of 65
151 modules (22% of all high-quality modules) were significantly enriched with nine of these TF
152 regulons (**Fig. 2B**). The EGRIN model recapitulated 541 of the 1,212 (45%) previously
153 characterized interactions. This value is consistent with the recall rate of the EGRIN model for *M.*

154 *tuberculosis* (41%-49%) (28). The poor recall of the remaining four regulons (141 regulatory
155 interactions) could be due to underrepresentation of gene expression data from relevant
156 conditions in which these regulons are conditionally active. This analysis also uncovered
157 combinatorial regulation of genes across 19 modules (i.e. enriched with more than one TF
158 regulon). Consistent with the known hierarchical scheme for regulation of sporulation (30),
159 expression of 161 genes across at least eight modules were putatively influenced by Spo0A in
160 combination with one or more alternative sigma factors implicated in sporulation (e.g., SigE).
161 EGRIN also predicted CcpA contributions in seven additional modules in combination with CodY,
162 PrdR and SigL, illustrating the complexity of modular transcriptional regulation in *C. difficile*.
163
164 The biclustering of genes by cMonkey2 is constrained by the *de novo* discovery of a conserved
165 GRE(s) within their promoters in order to cluster genes that are co-regulated, and not just co-
166 expressed. The GREs represent putative binding sites for TFs that are often independently
167 implicated by the Inferelator and protein-DNA interaction maps as regulators of genes within the
168 same module(28, 29, 31). Notably, we determined that the GREs within promoters of genes in
169 modules #182 and #309 were similar to known binding sites for CodY and SigL, which are
170 predicted regulators of those modules, and are among the very few TFs for which binding sites
171 have been characterized (**Fig. 2C-D**).
172
173 The EGRIN modules also detected co-regulation of genes within and across functionally related
174 operons. For example, module #152, which is enriched with the SigD regulon, contains 16 genes
175 that were part of four operons including the flagellar operon *flgG1G-fliMN*-CD630_02720-*htpG,* in
176 addition to *pyrBKDE*, CD630_30270-CD630_30280-*malY*-CD630_30300, and CD630_32430-
177 *prdA*. *De novo* search for TF motifs traditionally use dozens of sequences to identify putative
178 GREs. With the amount of transcriptomic information available, further robust prediction of
179 putative GREs was limited by available numbers of putative binding sites after genes were

180 organized into predicted operon structures. In addition, multiple modules with statistically
181 significant GREs could not be matched to characterized TFs due to the limited number of TFs
182 with known motifs in *C. difficile*. These limitations can be overcome with additional transcriptomic
183 datasets, as leveraged for EGRIN model development for other species.
184
185 ***C. difficile* EGRIN model uncovers regulatory networks for the Pathogenicity Locus**
186 We evaluated capacity for the EGRIN model to recall known mechanisms of PaLoc regulation,
187 and to provide new information regarding complex regulatory and small molecule effects. The
188 EGRIN model captured certain previously described effects of CodY on toxin gene expression
189 (**Fig. 2E**), as shown in module #182, which is enriched with members of the CodY regulon
190 including *tcdA*. In agreement with EGRIN-predicted CodY regulation of PaLoc genes in module
191 #182, genes encoding the toxin *tcdA* and its regulator *tcdR* were significantly overexpressed upon
192 deletion of *codY* (**Fig. 2G**). Interestingly, *tcdB* which was co-regulated with sporulation genes in
193 module #397 was also significantly upregulated in the *codY* deletion strain, suggesting that this
194 effect might be an indirect consequence of disrupted CodY regulation of *tcdR* (**Fig. 2G**). It is
195 assumed that CodY acts on PaLoc gene expression primarily through its repression of *tcdR.*
196 Putative lower affinity binding sites have been suggested in the toxin gene promoter regions (32).
197 The presence of the CodY motif (**Fig. 2C**) in most members of module #182, including *tcdA*
198 (purple font in **Fig. 2E**) suggests direct influence of CodY on *tcdA* gene expression. The EGRIN
199 model also identified previously reported connections between sporulation and toxin production
200 (33). *tcdB* was assigned to module #397, which was significantly enriched with genes controlled
201 by Spo0A, the master regulator of sporulation (**Fig. 2F**). Additional members of the PaLoc were
202 assigned to other modules, supporting the presence of multiple condition-dependent promoters
203 within the PaLoc (**Table S2**).
204
205 **Assignment of putative functions to genes in EGRIN modules**

206 Approximately 33% of gene features in the CD630 genome have unknown functions. Thus, the
207 *C. difficile* EGRIN model emerges as a resource to assign putative functions to uncharacterized
208 genes based on functional associations among co-regulated genes (i.e. guilt-by-association)(34).
209 We predicted putative functions for 48 uncharacterized genes by mining underlying functional
210 enrichment of modules under different experimental conditions (see methods). These 48
211 previously uncharacterized genes were associated with 13 functional categories, including
212 "Sporulation" and "Other sugar-family transporters" (**Fig. 3A**).
213
214 Ten genes were putatively assigned sporulation-related functions based on their co-regulation in
215 the sporulation associated modules #206 and #251 (**Fig. 3B)**. Module #251 includes the
216 sporulation-associated alternative sigma factors SigG and SigE (located in the same operon).
217 Module #206 includes seven stage III sporulation genes (*spoIIIAA*, *spoIIIAB*, *spoIIIAC*, *spoIIIAD*,
218 *spoIIIAF*, *spoIIIAG* and *spoIIIAH*), and two stage IV sporulation genes (*spoIV*, *spoIVA*). Reduced
219 expression of the 10 putative sporulation genes upon deletion of sporulation-associated sigma
220 factors suggested putative roles within the mother cell or the forespore. Seven genes are likely
221 associated with mother cell-specific roles based on their decreased expression in *sigE* (six genes)
222 and *sigK* (one gene) deletion strains (**Table S1**). Two additional genes were down-regulated in a
223 *sigG* deletion strain, suggesting putative functions in the forespore. Notably, Tn-seq studies for
224 gene essentiality in *C. difficile* identified seven of these 10 genes as required for sporulation (35).
225
226 Module #43 contains six genes, organized in a single operon (CD630_15840-15890), associated
227 with the category "Other Sugar-family transporters". Studies by Antunes et al. (3) identified
228 members of the CD630_15840-15890 operon to be regulated by glucose and indirectly by CcpA.
229 Thus, the 12 uncharacterized genes included in module #43 may also be associated with the
230 same functional category (**Fig. 3C**). Two of these uncharacterized genes (CD630_13011 and
231 CD630_29661) were also identified as CcpA targets in the presence of glucose (3). These

232 EGRIN-predicted functional assignments are consistent with the known role of CcpA in regulating
233 sugar transport and metabolism (3).
234
235 Module #48 contains two adjacent operons (*4hbd-cat2*-CD630_23400-*abf2* and *sucD-cat1*)
236 associated with aminobutanoate degradation. Both operons are regulated by CodY and PrdR.
237 Hence, we predicted that the four uncharacterized genes in this module may be also involved in
238 amino acid metabolism (**Fig. 3C**). In support of this hypothesis, CD630_08760 and CD630_08780
239 are both differentially expressed upon *codY* deletion. Recent studies also suggest that CD630_
240 08760 may function as a tyrosine transporter per its homology to the CodY-regulated neighbor
241 gene, CD630_08730 (36). Furthermore, Steglich et al. (37) observed decreases in tyrosine uptake
242 and Stickland fermentation in clinical isolates lacking CD630_08760 and CD630_08780.
243
244 **EGRIN uncovers differentially active regulatory networks during *in vivo* infection**
245 We investigated the differential expression of EGRIN modules across multiple published *in vivo*
246 experiments to discover underlying regulatory mechanisms that drive *C. difficile's* colonization
247 and adaption to *in vivo* environments. This analysis discovered the *in vivo* activation of module
248 #158, particularly during acute infection, and the down regulation of module #48; notably the latter
249 was upregulated during early infection (**Fig. 4A-B**). Module #48 is enriched with members of the
250 CodY and PrdR regulons, as described above. Module #158 is enriched for putative PrdR and
251 EutV co-regulated ethanolamine utilization genes, including *eut* operons for a 2-component
252 histidine kinase sensing system and carboxysome structural proteins that house the ethanolamine
253 fermentative enzymes (38). Ethanolamine is prevalent within gut secretions and is also released
254 from damaged host tissues, providing a readily available carbon and nitrogen source for *C.*
255 *difficile*. The predicted co-regulation of this gene module by PrdR suggests additional *in vivo*
256 functions of this regulator to optimize *C. difficile's* metabolism in gut environments.
257

258 With capacity to identify intestinal contributions to *C. difficile* responses we leveraged the EGRIN
259 model to analyze commensal modulation of the pathogen's virulence, using transcriptomic
260 datasets from gnotobiotic mice that were mono-colonized with the mouse-infective strain *C.*
261 *difficile* ATCC43255 or co-colonized with *C. difficile* and the protective gut commensal species
262 *Paraclostridium bifermentans* (PBI), or infection-worsening species *Clostridium sardiniense*
263 (CSAR). These datasets were not used in model construction. By mapping sets of differentially
264 expressed genes into the EGRIN model we uncovered modules across 20 cellular processes and
265 their associated TFs that were differentially regulated in the presence of PBI or CSAR (**Fig. 4C-**
266 **F**).
267
268 Two sporulation-enriched modules (modules #206 and #261) were up-regulated by 24h of
269 infection in monocolonized mice (**Fig. 4C**). The same two modules were up-regulated by 24h of
270 infection in CSAR co-colonized mice, in addition to four other modules also enriched with
271 sporulation genes (modules #82, #223, #242, #251 in **Fig. 4D**). These six modules were enriched
272 with the Spo0A regulon. On the other hand, no sporulation-enriched modules were detected by
273 24h of infection in PBI co-colonized mice (**Fig. 4E**). Comparison of CSAR co-colonized mice and
274 PBI co-colonized mice discovered four sporulation-enriched modules (including modules #206
275 and #261) with increased expression in the virulent context (i.e. presence of CSAR) (**Fig. 4F**).
276 These findings were confirmed with the high levels of spore release in expanded populations of
277 vegetative *C. difficile* when co-colonized with CSAR (22). Overall, this analysis suggested that
278 the sporulation pathway is an indicator of *C. difficile* disease, reinforcing the Spo0A-mediated link
279 between sporulation and toxin production recapitulated by the model (**Fig. 2F**).
280
281 Module #319 contains multiple genes associated with electron transport via Rnf ferredoxin
282 systems, and steps in glycolytic, butanoate and succinate metabolic pathways. This module was
283 upregulated at later stages of infection in monocolonized mice at 24h (**Fig. 4C**), and was also up-

284 regulated in CSAR co-colonized mice when compared to PBI co-colonized mice (**Fig. 4F**). Module
285 #319 was consistently down-regulated in mice co-colonized with the protective commensal PBI
286 (**Fig. 4E**). These findings show associated activation of multiple co-regulated energy generating
287 pathways in hypervirulent states of *C. difficile*. Because the EGRIN model identified the
288 NAD+/NADH sensing regulator Rex as a potential activator of module #319, the observed down-
289 regulation of module #319 in PBI co-colonized mice indicates decreased Rex activity. This may
290 explain why a *rex* deletion strain supported increased survival in hamsters (24).
291
292 Five modules enriched with the SigD-regulated genes encoding subunits of flagella (modules
293 #184, #187, #295, #296 and #358) were downregulated in monocolonized mice at 24h (**Fig. 4C**).
294 Similarly, two modules enriched with SigD-regulated motility genes (modules #152 and #295)
295 were downregulated in CSAR co-colonized mice (**Fig. 4D**). From these modules, only module
296 #152 was downregulated in PBI co-colonized mice (**Fig. 4E**), indicating that motility may be
297 repressed to redirect resources toward pathogenesis. This finding is supported by increased
298 virulence of *C. difficile* strains lacking a functional flagella (39). Surprisingly, module #273
299 enriched with the SigD regulon but not with flagellar genes was downregulated in PBI co-
300 colonized mice (**Fig. 4E**) but upregulated in CSAR co-colonized mice (**Fig. 4F**). One of the genes
301 in this module *luxS* encodes a protein involved in the synthesis of the quorum sensing signal, and
302 its over-expression increases toxin expression (40). While it is unclear whether SigD plays a role
303 in the expression of this module, these observations suggest that downregulation of module #
304 273 and *luxS* (through a still uncharacterized mechanism) may contribute to the PBI-mediated
305 reduction of *C. difficile* virulence. In summary, the described EGRIN modules illustrate the
306 potential of the model to uncover additional co-regulated genes and cellular functions that enable
307 states of enhanced virulence within *C. difficile*, and support multiple additional hypotheses for
308 experimental validation.
309

310 **Metabolic network analyses elucidate *in vivo* metabolic adaptations of *C. difficile***

311 To investigate how specific genes within *C. difficile* contribute to *in vivo* phenotypes needed to
312 develop symptomatic infection we leveraged reconstructed metabolic models that mapped
313 functionally annotated genes to curated biochemical reactions. We extended a previously
314 developed icdf834 metabolic model for *C. difficile* strain 630 (41, 42). The icdf834 model
315 incorporates 1227 metabolic reactions and 807 metabolites. The metabolic reactions were
316 mapped through gene-protein-reaction (GPR) associations to 834 genes, which represent 80%
317 of 1,030 identified metabolic genes in the CD630 genome (**Fig. 5A**). We increased the number of
318 genes in the icdf834 model from 834 to 838 (**Fig. 5B**), and added six new exchange reactions to
319 account for *C. difficile's* capacity to utilize mannitol, fructose, sorbitol, raffinose, succinate and
320 butanoate (43, 44) (**Fig. 5B**). We also added four genes (CD630_08700, CD630_08680,
321 CD630_17090 and CD630_10810) that encode three reactions for molybdenum utilization and
322 cofactor synthesis. Lastly, we updated pathway annotations to reflect those found in obligate
323 anaerobes. For example, the tricarboxylic citric acid cycle (TCA) is not found in most anaerobes,
324 though some reactions, in reverse, support aspects of pyruvate, succinate and oxaloacete
325 metabolism. In the icdf834 model, we changed subsystem pathway annotation of two reactions -
326 i) acetyl-CoA:oxaloacetate C-acetyltransferase and ii) succinyl-CoA synthase from TCA cycle to
327 pyruvate metabolism and butanoate fermentation respectively (**Supplementary File S1**). Similar
328 updates were performed for reactions originally assigned to gluconeogenesis and the pentose
329 phosphate pathway. We refer to this updated model as icdf838. Lastly, the model derived from
330 CD630 was compared with the gene feature content from *C. difficile* ATCC43255, used commonly
331 in mouse infection models. The two strains shared 92% of metabolic genes and predicted
332 pathways (768 out of 838 genes in the icdf838 model have homology with the ATCC43255 strain;
333 **Supplementary File S1**).
334

335 We validated the completeness and accuracy of this model by confirming its ability to predict
336 biomass production in three different *in vitro* media compositions: 1) minimal medium, 2) basal
337 defined medium and 3) complex, nutrient-rich medium (see Larocque et al. 2014 (42) for media
338 compositions). The model accurately predicted *C. difficile's* requirements for six amino acids:
339 cysteine, leucine, Isoleucine, proline, tryptophan and valine (45). We also tested the performance
340 of this "*in silico broth*" model for accuracy in predicting gene essentiality by comparing our model
341 predictions to results from Tn-seq fitness screen performed *in vitro* under nutrient-rich conditions
342 (35). With a threshold cutoff of 95% predicted growth inhibition, receiver-operator curve (ROC)
343 analyses demonstrated high sensitivity and specificity of the model predictions (**Fig. 5C**; area
344 under curve = 0.7626; p-value=0.015), indicating capacity for the model to distinguish essential
345 versus non-essential gene calls with a true positive rate (sensitivity) of 0.9791 and a false positive
346 rate (specificity) of 0.5431(**Fig. 5C**).
347
348 We next extended and applied the model to predict *C. difficile* behaviors and gene essentiality *in*
349 *vivo. C. difficile* transcriptomes from specifically-colonized gnotobiotic mice (22) were used as
350 input into the GIMME algorithm (46). Analyses of expressed transcripts *in vivo* identified 665
351 active reactions (**Fig. 5B**) within the icdf838 model during colonization, growth, and over the
352 course of symptomatic infection. Leveraging information from the *in vitro* studies, the model made
353 two notable predictions *in vivo* regarding the pathogen's metabolism. First, the icdf838 model
354 predicted 15 amino acids to be required for *C. difficile* growth in contrast to the 6 required *in vitro*
355 (**Supplementary File S1**). These amino acids included the dominant Stickland-fermented amino
356 acids that were also required *in vitro,* including proline and branched chain amino acids, and
357 additional amino acids including arginine, glutamate, lysine and methionine, which also have
358 multiple cellular functions in cell wall synthesis, nitrogen cycling, and responses to oxidative
359 stress. Secondly, the model predicted *C. difficile's* switch from preferential use of glucose as a
360 carbon source *in vitro* in complex media, to simultaneous utilization *in vivo* of diverse carbohydrate

361 sources including fructose, galactose, maltose, and sugar alcohols such as mannitol and sorbitol,
362 to promote colonization and growth (**Supplementary File S1**). Seven of these carbohydrate
363 sources were described in other *in vivo* mouse infection studies illustrating support for these
364 findings across *C. difficile* strains, and in germfree and conventional mouse models
365 (**Supplementary File S1**) (43, 44, 47).
366
367 We next used the metabolic model to identify essential metabolic genes and networks that
368 promote *C. difficile's* growth *in vivo*. Gene deletions predicted to reduce the pathogen's *in vivo*
369 growth by ≥95% identified 24 genes, involved in 1 carbon-cycling reactions in glyoxylate and
370 Wood-Ljungdahl metabolism, nucleotide biosynthesis, nucleotide interconversion and salvage
371 pathways, amino acid biosynthetic and metabolic reactions, and aspects of central carbohydrate
372 metabolism (**Fig. 5D-E**). These metabolic pathways represent new potential targets that drive
373 aspects of *C. difficile's* colonization and subsequent growth which are required to develop
374 symptomatic infections. Model predictions also illustrated *C. difficile's* predicted shift from
375 carbohydrate utilization towards amino acid utilizing pathways *in vivo*, as shown by the enhanced
376 set of 15 amino acids, including the preferred Stickland donor and acceptor amino acids (leucine
377 and proline) known to support metabolism and growth (43, 44, 47). Notably, many of these amino
378 acids show high abundance within the gut lumen in gnotobiotic and conventional colonization
379 states that enhance *C. difficile's* capacity to colonize and expand (22).
380
381 **The Cdiff Web Portal, a resource for the *C. difficile* community**
382 We have released a new *C. difficile* Web Portal (http://networks.systemsbiology.net/cdiff-portal/)
383 to provide a discovery and collaboration gateway for the *C. difficile* scientific community. The
384 portal aims to accelerate the advancement of the science and understanding of *C. difficile* biology,
385 gene regulation, and metabolism on its virulence. Within the portal users can access publicly

386 available datasets (e.g. transcriptional compendia), models, software and supporting resources.
387 The Portal includes information on more than 4,000 *C. difficile* genes, 1,227 metabolic reactions,
388 and 406 co-regulated gene modules. Genes can be explored in the context of genome
389 annotations, expression profiles, regulatory and metabolic membership, and other functional
390 genomic information across different databases including COG, Uniprot, and PATRIC (48–50).
391 The portal provides access to detailed information on (1) Genes, (2) predicted Gene Modules,
392 and (3) Metabolic Reactions (**Fig. S2**).
393
394 Each gene module page includes summary statistics for the module, expression profiles of the
395 module genes across conditions incorporated in developing the model, regulatory motifs,
396 regulatory influences from transcription factors, functional enrichment information, and
397 information about regulon member genes (**Fig. 6**). The module pages are structured to facilitate
398 the assessment of the quality and statistical significance of the modules and highlight functional
399 connections. The portal includes a table of metabolic reactions with details of each reaction,
400 associated genes, metabolites, and sub-systems. Metabolites and sub-systems are defined as
401 taxonomic vocabularies that collect and group associated reactions to identify related metabolic
402 processes. In addition, the portal provides access to algorithms, software, and data, and will
403 include information about animal models, strains, and other *C. difficile* relevant community
404 resources. As additional datasets are communicated, model predictions and tools will be
405 successively enhanced to support systems-level analyses and assist in hypothesis generation in
406 *C. difficile* biology and to enable tangible clinical interventions.
407

408 **DISCUSSION**

409 The obligate anaerobe *C. difficile* is unique among gut anaerobes in possessing a diverse carbon
410 source metabolism to enable colonization and growth in gut environments. These systems further
411 exist within a complex network of gene regulatory modules that modulate growth, energy balance,
412 and stress responses *in vivo*. Capacity to understand these systems-level integration points has
413 remained challenging in the absence of robust systems biology models to infer *C. difficile's in vivo*
414 behaviors. We acknowledge the detailed studies from multiple groups over prior decades that
415 provided a critical mass of information on *C. difficile's* nutrient and gene-level responses to
416 support development of an EGRIN model, the first for a gut anaerobe and toxigenic species. We
417 emphasize that this information, the most for any obligate anaerobe, still represents a small
418 fraction of that normally used to develop thorough EGRIN models. Recent improvements in the
419 genetic manipulation of *C. difficile*, including the mouse infective strain ATCC43255, open new
420 capacity to probe the GREs modulating critical aspects of its metabolism, growth and virulence,
421 from a systems-level perspective.

422

423 The *C. difficile* EGRIN model enables a number of predictions relevant to *in vivo* disease. For
424 example, the PrdR regulator of the pathogen's Stickland proline reductase (*prd*) and other genes,
425 has long been hypothesized to have a role in PaLoc gene expression through as-yet unknown
426 mechanisms. EGRIN predictions included gene regulatory module #182 which identified
427 combined PrdR and CodY effects on *tcdA* gene expression, providing a regulatory integration
428 point and broader set of co-regulated genes to support further experimental analyses of co-
429 regulation between these two transcription factors, including effects on PaLoc expression.
430 Biclustering also identified interactions between Spo0A, another regulator hypothesized to
431 modulate PaLoc expression, and *tcdB* expression in module #397. The identified modules,
432 associated genes and regulators provide new information to support further experimental

433 investigation of combinatorial effects of these and other regulators identified in PaLoc gene-
434 associated biclusters. The EGRIN model also predicted PrdR as a critical regulator *in vivo* through
435 its systems-level effects on the pathogen's colonization, metabolism and growth, involving
436 multiple direct and indirect effects upon other modules and aspects of the pathogen's metabolism
437 and gene regulation.
438
439 The present model did not identify all experimentally known regulators of PaLoc expression,
440 including SigD regulation of TcdR, and effects of other more recently identified PaLoc regulators
441 such as RstA and LexA, for which limited datasets exist from targeted deletion mutants or under
442 multiple nutrient and other environmental perturbations. Nonetheless, as shown with our *in vivo*
443 analyses, application of the EGRIN and metabolic models to new datasets offers key insights into
444 causal mechanistic drivers of adaptive strategies of the pathogen. Given that less than 10% of
445 transcriptomic information and less than 1% of ChIP-seq regulator datasets were available for *C.*
446 *difficile* 630, as compared to EGRIN models developed for other species*,* the model provides a
447 formative tool to design future transcriptomic and ChIP-seq studies to improve predictions for
448 these regulons.
449
450 Leveraging additional Tn-seq and *in vivo* transcriptomic datasets, the expanded icdf838 model
451 identified a broader set of amino acids, in addition to genes and anaerobe-specific pathways,
452 needed to support colonization and growth expansion *in vivo*. Notably, predictions of *in vivo* gene
453 essentially identified multiple genes in glyoxylate metabolism, a pathway essential in many
454 acetogenic anaerobes (51, 52) that leverage this system with folate 1-carbon cycling pathways
455 including those connected with Wood-Ljundahl fixation of carbon dioxide to acetate. Predictions
456 of gene essentiality also identified multiple nucleotide synthesis and salvage pathway genes that
457 were essential *in vivo* but not *in vitro,* including ones associated with xanthine transport and
458 metabolism, an abundant nucleotide in gut secretions that originates from host sources (22).

459 Lastly, predictions identified genes in amino acid biosynthetic pathways for branched-chain amino
460 acids, aromatic amino acids, and others that were predicted to be required *in vivo.* Each of these
461 provides new targets of vulnerability for which to consider therapeutic interventions leveraging
462 small molecules, bacteriotherapeutic, or other patient interventions.
463
464 We illustrate additional predictions from the *C. difficile* EGRIN model to enable gene- through
465 systems-level analyses of the pathogen. Though among the best described obligate anaerobes,
466 the *C. difficile* genome still contains a high number of genes of unknown function. Model
467 predictions provided new information to assign putative functions to 48 gene features, including
468 ones associated with sporulation, carbohydrate transport, and other aspects of cellular
469 metabolism. The *C. difficile* Web Portal, makes these tools and resources available to the broader
470 *C. difficile,* microbiology, and systems biology communities, providing a platform for collaboration
471 and to support systems-level investigations of the pathogen and its interactions with the host and
472 commensal microbiota.
473
474
475
476

477 # METHODS

478 ***C. difficile* genome annotation**

479 A new ATCC43255 reference genome was generated and annotated to support *in vivo*
480 transcriptome studies of *C. difficile* per discrepancies noted in the RefSeq genome, particularly
481 among bacteriophage loci and other mobile elements (22). The updated reference genome was
482 annotated using the NCBI Prokaryotic Genome Automatic Annotation Pipeline (53), PATRIC (50),
483 and PROKKA (54) to extract gene features for support of transcriptome pathway enrichment
484 analyses. Bacteriophage loci and genes were identified using PHASTER (55).

485

486 ***C. difficile* transcriptional compendium**

487 To generate a transcriptional compendium for *C. difficile*, required for constructing an EGRIN
488 model, a total of 148 publicly available transcriptomes of *C. difficile* 630 were downloaded from
489 the NCBI Gene Expression Omnibus (GEO) repository (56) in March 2020. Downloaded
490 transcriptomes were generated by 11 independent studies (**Table 1**). To integrate this data into a
491 single dataset, we computed the log2 fold-change of each transcriptome with respect to a control
492 condition, as performed in the generation of other transcriptional compendia (57). This step was
493 not necessary for transcriptional data collected with dual channel arrays that included a
494 normalizing control channel. The resulting transcriptional compendium contained a total of 4,091
495 gene features and 127 conditions. The 127 conditions in the transcriptional compendium were
496 organized in 10 distinct conditional blocks (e.g. sporulation, *fur* deletion), as shown in **Table 1**.

497

498 **Construction of the EGRIN model**

499 The EGRIN model for *C. difficile* was constructed in two stages. First, we used cMonkey2 (26), a
500 biclustering algorithm, on the compiled compendium of 127 *C. difficile* transcriptomes to
501 simultaneously detect co-regulated gene modules and the conditions where co-regulation occurs.

502 cMonkey2 integrates functional annotation from the STRING database (25), gene promoter
503 sequences from the RSAT database (58), and operon predictions from MicrobesOnline (59) when
504 detecting the gene modules. cMonkey2 was run using default parameters. Briefly, we used 2,000
505 iterations to optimize the co-regulated gene modules, each one with 3-70 genes. In each iteration,
506 cMonkey2 refined the gene modules by evaluating and modifying (if necessary) condition and
507 gene memberships. cMonkey2 biclustering approach allowed genes and conditions to be
508 assigned to a maximum of two and 204 different modules, respectively. *De novo* motif search was
509 performed using MEME v. 4.12.0 (60). Second, we used the Inferelator (27), a network inference
510 algorithm, to identify potential transcriptional regulators for the 406 gene modules generated by
511 cMonkey2. The Inferelator uses a Bayesian best subset regression to estimate the magnitude
512 and sign (activation or repression) of potential interactions between TFs and gene modules. We
513 bootstrapped the expression data (20 times) to avoid regression overfitting (27). The Inferelator
514 generates two scores for each TF-module interaction, the corresponding regression coefficient
515 and a confidence score. The second score indicates the likelihood of the interaction. The final set
516 of TF-module interactions was defined as the 704 interactions with the top 10% of highest non-
517 zero confidence scores.
518
519 **Experimentally supported literature derived TF regulons**
520 We mined available literature to compile a list of experimentally supported targets for the 13
521 partially characterized transcriptional regulators (involved in sporulation, motility, carbon
522 metabolism, among other processes) shown on **Table S1**. The manually compiled regulons
523 represented a total of 1,353 regulatory interactions and involved 1,050 genes. Target genes
524 included in the compiled TF regulons were supported by transcriptional data, protein-dna binding
525 data and *in silico* analysis of promoter regions (e.g. presence of known regulators DNA binding
526 motif).
527 **Module enrichment evaluation**

528 We used a hypergeometric test to identify modules of co-regulated genes in the EGRIN model
529 that were statistically enriched with manually compiled TF regulons (**Table S1**) or functional
530 pathways derived from curated annotation of *C. difficile* genome (22). Only gene modules with
531 adjusted hypergeometric test p-value ≤ 0.05 and containing four or more genes from the relevant
532 TF regulon or functional pathway were considered enriched.
533
534 **Analysis of *in vivo* data**
535 *In vivo* transcriptomic data from gnotobiotic mice monocolonized with *C. difficile* ATCC43255 or
536 co-colonized with *P. bifermentans* or *C. sardiniense* were analyzed as described (22) using the
537 updated reference genome of ATCC43255 to extract gene features for subsequent analysis with
538 DESEQ2.
539
540 **Metabolic model refinement and gene essentiality prediction**
541 A published genome-scale metabolic model of *C. difficile* 630 strain, icdf834 (41), was used in
542 this study and expanded by adding reactions required for *in vivo* survival of the pathogen. We
543 also curated pathway annotations that were incorrectly designated using default KEGG
544 annotations (61). For example, the TCA, gluconeogenesis and pentose phosphate pathways are
545 incomplete in *C. difficile*. Thus, we updated the annotation of these pathways as part of pyruvate
546 metabolism, butanoate fermentation and Galactose & Tagatose metabolism (**Supplementary**
547 **File S1**). Initially, we evaluated the homology of metabolic genes between *C. difficile* 630 and
548 ATCC43255 strain of *C. difficile* in order to use the icdf834 model for representing the *in vivo*
549 infection state of ATCC43255 strain. The details of 764 genes that are predicted in this homology
550 analysis is provided in **Supplementary File S1**. Then, the transcriptome of *C. difficile* profiled
551 from *in vivo* infections of specifically-colonized gnotobiotic mice (22) was mapped onto the icdf834
552 model using the GIMME algorithm (46). This resulted in a model with 665 active reactions, with
553 no changes in the number of genes. We then expanded the model by including four new genes

554 and 8 new reactions (**Supplementary File S1**) that are required for the growth of the pathogen in
555 the *in vivo* micro-environment, based on KEGG annotations. We named this expanded version of
556 the model as "icdf838". This model represents the *in vivo* state of *C. difficile*. We then applied the
557 constraint-based method for simulating the metabolic steady-state of *C. difficile* using flux-balance
558 analysis (FBA) (46, 62). The initial validation steps involved checking the capacity of the icdf834
559 model to produce biomass in defined media conditions including 1) minimal medium, 2) basal
560 defined medium and 3) complex, nutrient-rich medium (compositions used according to Larocque
561 et al 2014 (42)). Then, we tested the performance of the icdf834 model using gene essentiality
562 predictions by FBA. A gene was considered "essential" if its deletion reduced the biomass by
563 >95%. By this analysis, the model classified each gene as "essential" or "non-essential". We
564 compared the gene essentiality predictions from nutrient-rich media constraints with the available
565 experimental Tn-seq data (35) and deduced the confusion matrix to derive true positive rates
566 (TPR) and false positive rates (FPR). This led to the elucidation of sensitivity and specificity of the
567 model using ROC curve analysis. We then applied the same strategy and predicted the essential
568 genes *in vivo* using FBA with the expanded context-specific network, icdf838. All model
569 simulations related to FBA were performed on MATLAB_R2019a platform using the recent
570 version of COBRA (The COnstraint-Based Reconstruction and Analysis) toolbox (63). *In silico*
571 gene essentiality predictions were performed using the COBRA toolbox 'single-gene-deletion'
572 function in MATLAB. The illustration of essential gene regulatory network *in vivo* was deduced
573 using BioTapsetry tool (http://www.biotapestry.org/).
574

575 ***C. difficile* Web Portal**

576 This portal utilizes the powerful build, search, collaboration, and visualization features of the
577 Drupal content management system. With the two key features of modularity and extensibility,
578 Drupal provides a slim, powerful core that can be readily extended through custom modules and
579 easy-to-use collaborative tools to support information sharing. Based on these key features, we

580 developed this content management system into a data management, analysis, and visualization
581 framework to support *C. difficile* research.
582
583 Due to the complexity of the information provided by the genome and models, it is critical to
584 provide a user-friendly and flexible search and filtering capabilities. By taking advantage of
585 Drupal's built-in search interface and implementing Apache Solr search, we created very powerful
586 search capabilities that will query every information included in the portal database. Moreover,
587 the search interface uses "facets" to allow users to explore a collection of information by applying
588 multiple filters. This combination together with sorting enables users to start with broad searches
589 and then quickly pinpoint specific information.
590
591 In order to provide a comprehensive functional genomics resource for the Cdiff community,
592 genome annotations from several different sources were merged and imported into the Cdiff
593 Portal. Curated genome annotations for *Clostridium difficile* strain 630 published by Monot et al.
594 (21), were downloaded from MicroScope platform (64). Additional functional annotations were
595 downloaded from PATRIC (50) and Uniprot (49) and merged with curated genome annotations.
596 Overall, 4,018 genes were included in the Cdiff Portal. The *C. difficile* genome included 1,030
597 metabolic genes, 309 TFs, 270 sRNAs, 87 tRNAs, 32 rRNAs and 17 miscRNAs. The genome
598 included 1,330 genes with unknown function. Furthermore, gene essentiality data from Dembek
599 et al. (35) was integrated with gene annotations.
600
601

602 **REFERENCES**

603

604 1. Monegro AF, Regunath H. 2018. Hospital acquired infectionsStatPearls. StatPearls
605 Publishing.
606 2. Aktories K. 2011. Bacterial protein toxins that modify host regulatory GTPases. Nat Rev
607 Microbiol 9:487–498.
608 3. Antunes A, Camiade E, Monot M, Courtois E, Barbut F, Sernova N V, Rodionov DA,
609 Martin-Verstraete I, Dupuy B. 2012. Global transcriptional control by glucose and carbon
610 regulator CcpA in Clostridium difficile. Nucleic Acids Res 40:10701–10718.
611 4. Saujet L, Monot M, Dupuy B, Soutourina O, Martin-Verstraete I. 2011. The key sigma
612 factor of transition phase, SigH, controls sporulation, metabolism, and virulence factor
613 expression in Clostridium difficile. J Bacteriol 193:3186–3196.
614 5. Matamouros S, England P, Dupuy B. 2007. Clostridium difficile toxin expression is
615 inhibited by the novel regulator TcdC. Mol Microbiol 64:1274–1288.
616 6. Mani N, Dupuy B. 2001. Regulation of toxin synthesis in Clostridium difficile by an
617 alternative RNA polymerase sigma factor. Proc Natl Acad Sci 98:5844–5849.
618 7. Smits WK, Lyras D, Lacy DB, Wilcox MH, Kuijper EJ. 2016. Clostridium difficile infection.
619 Nat Rev Dis Prim 2:1–20.
620 8. Lyon SA, Hutton ML, Rood JI, Cheung JK, Lyras D. 2016. CdtR regulates TcdA and TcdB
621 production in Clostridium difficile. PLoS Pathog 12:e1005758.
622 9. Walter BM, Rupnik M, Hodnik V, Anderluh G, Dupuy B, Paulič N, Žgur-Bertok D, Butala
623 M. 2014. The LexA regulated genes of the Clostridium difficile. BMC Microbiol 14:88.
624 10. Edwards AN, Tamayo R, McBride SM. 2016. A novel regulator controls C lostridium
625 difficile sporulation, motility and toxin production. Mol Microbiol 100:954–971.
626 11. Martin-Verstraete I, Peltier J, Dupuy B. 2016. The regulatory networks that control
627 Clostridium difficile toxin synthesis. Toxins (Basel) 8:153.
628 12. Bradshaw WJ, Kirby JM, Roberts AK, Shone CC, Acharya KR. 2017. The molecular
629 structure of the glycoside hydrolase domain of Cwp19 from Clostridium difficile. FEBS J
630 284:4343–4357.
631 13. Woods EC, Nawrocki KL, Suárez JM, McBride SM. 2016. The Clostridium difficile Dlt
632 pathway is controlled by the extracytoplasmic function sigma factor $σ$V in response to
633 lysozyme. Infect Immun 84:1902–1916.
634 14. Neumann-Schaal M, Metzendorf NG, Troitzsch D, Nuss AM, Hofmann JD, Beckstette M,
635 Dersch P, Otto A, Sievers S. 2018. Tracking gene expression and oxidative damage of
636 O2-stressed Clostridioides difficile by a multi-omics approach. Anaerobe 53:94–107.
637 15. Kint N, Janoir C, Monot M, Hoys S, Soutourina O, Dupuy B, Martin-Verstraete I. 2017.
638 The alternative sigma factor $σ$B plays a crucial role in adaptive strategies of
639 Clostridium difficile during gut infection. Environ Microbiol 19:1933–1958.
640 16. Elena SF, Lenski RE. 2003. Evolution experiments with microorganisms: the dynamics
641 and genetic bases of adaptation. Nat Rev Genet 4:457–469.
642 17. Brooks AN, Turkarslan S, Beer KD, Yin Lo F, Baliga NS. 2011. Adaptation of cells to new
643 environments. Wiley Interdiscip Rev Syst Biol Med 3:544–561.
644 18. McDonald JAK, Mullish BH, Pechlivanis A, Liu Z, Brignardello J, Kao D, Holmes E, Li J V,
645 Clarke TB, Thursz MR, others. 2018. Inhibiting growth of Clostridioides difficile by
646 restoring valerate, produced by the intestinal microbiota. Gastroenterology 155:1495–
647 1507.
648 19. Vemuri RC, Gundamaraju R, Shinde T, Eri R. 2017. Therapeutic interventions for gut
649 dysbiosis and related disorders in the elderly: antibiotics, probiotics or faecal microbiota
650 transplantation? Benef Microbes 8:179–192.
651 20. Riedel T, Bunk B, Thürmer A, Spröer C, Brzuszkiewicz E, Abt B, Gronow S, Liesegang H,

652 Daniel R, Overmann J. 2015. Genome resequencing of the virulent and multidrug-
653 resistant reference strain Clostridium difficile 630. Genome Announc 3:e00276--15.
654 21. Monot M, Boursaux-Eude C, Thibonnier M, Vallenet D, Moszer I, Medigue C, Martin-
655 Verstraete I, Dupuy B. 2011. Reannotation of the genome sequence of Clostridium
656 difficile strain 630.
657 22. Girinathan BP, DiBenedetto N, Worley JN, Peltier J, Lavin Ri, Delaney ML, Cummins C,
658 Onderdonk AB, Gerber GK, Dupuy B, others. 2020. The mechanisms of in vivo
659 commensal control of Clostridioides difficile virulence. bioRxiv.
660 23. Bouillaut L, Self WT, Sonenshein AL. 2013. Proline-dependent regulation of Clostridium
661 difficile Stickland metabolism. J Bacteriol 195:844–854.
662 24. Bouillaut L, Dubois T, Francis MB, Daou N, Monot M, Sorg JA, Sonenshein AL, Dupuy B.
663 2019. Role of the global regulator Rex in control of NAD+-regeneration in Clostridioides
664 (Clostridium) difficile. Mol Microbiol 111:1671–1688.
665 25. Szklarczyk D, Morris JH, Cook H, Kuhn M, Wyder S, Simonovic M, Santos A, Doncheva
666 NT, Roth A, Bork P, others. 2016. The STRING database in 2017: quality-controlled
667 protein--protein association networks, made broadly accessible. Nucleic Acids Res
668 gkw937.
669 26. Reiss DJ, Plaisier CL, Wu W-J, Baliga NS. 2015. cMonkey2: Automated, systematic,
670 integrated detection of co-regulated gene modules for any organism. Nucleic Acids Res
671 43:e87.
672 27. Arrieta-Ortiz ML, Hafemeister C, Bate AR, Chu T, Greenfield A, Shuster B, Barry SN,
673 Gallitto M, Liu B, Kacmarczyk T, Santoriello F, Chen J, Rodrigues CD, Sato T, Rudner
674 DZ, Driks A, Bonneau R, Eichenberger P. 2015. An experimentally supported model of
675 the Bacillus subtilis global transcriptional regulatory network. Mol Syst Biol 11.
676 28. Peterson EJR, Reiss DJ, Turkarslan S, Minch KJ, Rustad T, Plaisier CL, Longabaugh
677 WJR, Sherman DR, Baliga NS. 2014. A high-resolution network model for global gene
678 regulation in Mycobacterium tuberculosis. Nucleic Acids Res 42:11291–11303.
679 29. Brooks AN, Reiss DJ, Allard A, Wu W-J, Salvanha DM, Plaisier CL, Chandrasekaran S,
680 Pan M, Kaur A, Baliga NS. 2014. A system-level model for the microbial regulatory
681 genome. Mol Syst Biol 10:740–740.
682 30. Saujet L, Pereira FC, Serrano M, Soutourina O, Monot M, Shelyakin P V, Gelfand MS,
683 Dupuy B, Henriques AO, Martin-Verstraete I. 2013. Genome-wide analysis of cell type-
684 specific gene transcription during spore formation in Clostridium difficile. PLoS Genet
685 9:e1003756.
686 31. Bonneau R, Facciotti MT, Reiss DJ, Schmid AK, Pan M, Kaur A, Thorsson V, Shannon P,
687 Johnson MH, Bare JC, Longabaugh W, Vuthoori M, Whitehead K, Madar A, Suzuki L,
688 Mori T, Chang D-E, Diruggiero J, Johnson CH, Hood L, Baliga NS. 2007. A predictive
689 model for transcriptional control of physiology in a free living cell. Cell 131:1354–65.
690 32. Dineen SS, Villapakkam AC, Nordman JT, Sonenshein AL. 2007. Repression of
691 Clostridium difficile toxin gene expression by CodY. Mol Microbiol 66:206–219.
692 33. Underwood S, Guan S, Vijayasubhash V, Baines SD, Graham L, Lewis RJ, Wilcox MH,
693 Stephenson K. 2009. Characterization of the sporulation initiation pathway of Clostridium
694 difficile and its role in toxin production. J Bacteriol 191:7296–7305.
695 34. Wolfe CJ, Kohane IS, Butte AJ. 2005. Systematic survey reveals general applicability of"
696 guilt-by-association" within gene coexpression networks. BMC Bioinformatics 6:227.
697 35. Dembek M, Barquist L, Boinett CJ, Cain AK, Mayho M, Lawley TD, Fairweather NF,
698 Fagan RP. 2015. High-throughput analysis of gene essentiality and sporulation in
699 Clostridium difficile. MBio 6:e02383--14.
700 36. Bradshaw WJ, Bruxelle J-F, Kovacs-Simon A, Harmer NJ, Janoir C, Péchiné S, Acharya
701 KR, Michell SL. 2019. Molecular features of lipoprotein CD0873: A potential vaccine
702 against the human pathogen Clostridioides difficile. J Biol Chem 294:15850–15861.

703 37. Steglich M, Hofmann JD, Helmecke J, Sikorski J, Spröer C, Riedel T, Bunk B, Overmann
704 J, Neumann-Schaal M, Nübel U. 2018. Convergent loss of ABC transporter genes from
705 Clostridioides difficile genomes is associated with impaired tyrosine uptake and p-cresol
706 production. Front Microbiol 9:901.
707 38. Nawrocki KL, Wetzel D, Jones JB, Woods EC, McBride SM. 2018. Ethanolamine is a
708 valuable nutrient source that impacts Clostridium difficile pathogenesis. Environ Microbiol
709 20:1419–1435.
710 39. Dingle TC, Mulvey GL, Armstrong GD. 2011. Mutagenic analysis of the Clostridium
711 difficile flagellar proteins, FliC and FliD, and their contribution to virulence in hamsters.
712 Infect Immun 79:4061–4067.
713 40. Lee ASY, Song KP. 2005. LuxS/autoinducer-2 quorum sensing molecule regulates
714 transcriptional virulence gene expression in Clostridium difficile. Biochem Biophys Res
715 Commun 335:659–666.
716 41. Kashaf SS, Angione C, Lió P. 2017. Making life difficult for Clostridium difficile:
717 augmenting the pathogen's metabolic model with transcriptomic and codon usage data
718 for better therapeutic target characterization. BMC Syst Biol 11:25.
719 42. Larocque M, Chénard T, Najmanovich R. 2014. A curated C. difficile strain 630 metabolic
720 network: prediction of essential targets and inhibitors. BMC Syst Biol 8:117.
721 43. Theriot CM, Koenigsknecht MJ, Carlson Jr PE, Hatton GE, Nelson AM, Li B, Huffnagle
722 GB, Li JZ, Young VB. 2014. Antibiotic-induced shifts in the mouse gut microbiome and
723 metabolome increase susceptibility to Clostridium difficile infection. Nat Commun 5:3114.
724 44. Janoir C, Denève C, Bouttier S, Barbut F, Hoys S, Caleechum L, Chapetón-Montes D,
725 Pereira FC, Henriques AO, Collignon A, others. 2013. Adaptive strategies and
726 pathogenesis of Clostridium difficile from in vivo transcriptomics. Infect Immun 81:3757–
727 3769.
728 45. Karasawa T, Ikoma S, Yamakawa K, Nakamura S. 1995. A defined growth medium for
729 Clostridium difficile. Microbiology 141:371–375.
730 46. Becker SA, Palsson BO. 2008. Context-specific metabolic networks are consistent with
731 experiments. PLoS Comput Biol 4:e1000082.
732 47. Jenior ML, Leslie JL, Young VB, Schloss PD. 2017. Clostridium difficile colonizes
733 alternative nutrient niches during infection across distinct murine gut microbiomes.
734 Msystems 2.
735 48. Galperin MY, Makarova KS, Wolf YI, Koonin E V. 2015. Expanded microbial genome
736 coverage and improved protein family annotation in the COG database. Nucleic Acids
737 Res 43:D261--D269.
738 49. Consortium TU. 2017. UniProt: the universal protein knowledgebase. Nucleic Acids Res
739 45:D158--D169.
740 50. Wattam AR, Abraham D, Dalay O, Disz TL, Driscoll T, Gabbard JL, Gillespie JJ, Gough
741 R, Hix D, Kenyon R, others. 2014. PATRIC, the bacterial bioinformatics database and
742 analysis resource. Nucleic Acids Res 42:D581--D591.
743 51. Gößner AS, Picardal F, Tanner RS, Drake HL. 2008. Carbon metabolism of the
744 moderately acid-tolerant acetogen Clostridium drakei isolated from peat. FEMS Microbiol
745 Lett 287:236–242.
746 52. Sakai S, Inokuma K, Nakashimada Y, Nishio N. 2008. Degradation of glyoxylate and
747 glycolate with ATP synthesis by a thermophilic anaerobic bacterium, Moorella sp. strain
748 HUC22-1. Appl Environ Microbiol 74:1447–1452.
749 53. Tatusova T, DiCuccio M, Badretdin A, Chetvernin V, Nawrocki EP, Zaslavsky L,
750 Lomsadze A, Pruitt KD, Borodovsky M, Ostell J. 2016. NCBI prokaryotic genome
751 annotation pipeline. Nucleic Acids Res 44:6614–6624.
752 54. Seemann T. 2014. Prokka: rapid prokaryotic genome annotation. Bioinformatics
753 30:2068–2069.

754 55. Arndt D, Grant JR, Marcu A, Sajed T, Pon A, Liang Y, Wishart DS. 2016. PHASTER: a
755 better, faster version of the PHAST phage search tool. Nucleic Acids Res 44:W16--W21.
756 56. Barrett T, Wilhite SE, Ledoux P, Evangelista C, Kim IF, Tomashevsky M, Marshall KA,
757 Phillippy KH, Sherman PM, Holko M, others. 2012. NCBI GEO: archive for functional
758 genomics data sets—update. Nucleic Acids Res 41:D991--D995.
759 57. Moretto M, Sonego P, Dierckxsens N, Brilli M, Bianco L, Ledezma-Tejeida D, Gama-
760 Castro S, Galardini M, Romualdi C, Laukens K, Collado-Vides J, Meysman P, Engelen K.
761 2016. COLOMBOS v3.0: leveraging gene expression compendia for cross-species
762 analyses. Nucleic Acids Res 44:D620-3.
763 58. Nguyen NTT, Contreras-Moreira B, Castro-Mondragon JA, Santana-Garcia W, Ossio R,
764 Robles-Espinoza CD, Bahin M, Collombet S, Vincens P, Thieffry D, others. 2018. RSAT
765 2018: regulatory sequence analysis tools 20th anniversary. Nucleic Acids Res 46:W209--
766 W214.
767 59. Dehal PS, Joachimiak MP, Price MN, Bates JT, Baumohl JK, Chivian D, Friedland GD,
768 Huang KH, Keller K, Novichkov PS, Dubchak IL, Alm EJ, Arkin AP. 2010.
769 MicrobesOnline: an integrated portal for comparative and functional genomics. Nucleic
770 Acids Res 38:D396-400.
771 60. Bailey TL, Johnson J, Grant CE, Noble WS. 2015. The MEME suite. Nucleic Acids Res
772 43:W39--W49.
773 61. Kanehisa M, Furumichi M, Tanabe M, Sato Y, Morishima K. 2017. KEGG: new
774 perspectives on genomes, pathways, diseases and drugs. Nucleic Acids Res 45:D353--
775 D361.
776 62. Orth JD, Thiele I, Palsson BØ. 2010. What is flux balance analysis? Nat Biotechnol
777 28:245–248.
778 63. Heirendt L, Arreckx S, Pfau T, Mendoza SN, Richelle A, Heinken A, Haraldsdóttir HS,
779 Wachowiak J, Keating SM, Vlasov V, others. 2019. Creation and analysis of biochemical
780 constraint-based models using the COBRA Toolbox v. 3.0. Nat Protoc 14:639–702.
781 64. Vallenet D, Calteau A, Cruveiller S, Gachet M, Lajus A, Josso A, Mercier J, Renaux A,
782 Rollin J, Rouy Z, others. 2017. MicroScope in 2017: an expanding and evolving
783 integrated resource for community expertise of microbial genomes. Nucleic Acids Res
784 45:D517--D528.
785 65. Dineen SS, McBride SM, Sonenshein AL. 2010. Integration of metabolism and virulence
786 by Clostridium difficile CodY. J Bacteriol 192:5350–5362.
787 66. Soutourina O, Dubois T, Monot M, Shelyakin P V, Saujet L, Boudry P, Gelfand MS,
788 Dupuy B, Martin-Verstraete I. 2020. Genome-Wide Transcription Start Site Mapping and
789 Promoter Assignments to a Sigma Factor in the Human Enteropathogen Clostridioides
790 difficile. Front Microbiol 11:1939.
791 67. Antunes A, Martin-Verstraete I, Dupuy B. 2011. CcpA-mediated repression of Clostridium
792 difficile toxin gene expression. Mol Microbiol 79:882–899.
793 68. Dubois T, Dancer-Thibonnier M, Monot M, Hamiot A, Bouillaut L, Soutourina O, Martin-
794 Verstraete I, Dupuy B. 2016. Control of Clostridium difficile physiopathology in response
795 to cysteine availability. Infect Immun 84:2389–2405.
796 69. Berges M, Michel A-M, Lassek C, Nuss AM, Beckstette M, Dersch P, Riedel K, Sievers S,
797 Becher D, Otto A, others. 2018. Iron regulation in Clostridioides difficile. Front Microbiol
798 9:3183.
799 70. El Meouche I, Peltier J, Monot M, Soutourina O, Pestel-Caron M, Dupuy B, Pons J-L.
800 2013. Characterization of the SigD regulon of C. difficile and its positive control of toxin
801 production through the regulation of tcdR. PLoS One 8.
802 71. Fimlaid KA, Bond JP, Schutz KC, Putnam EE, Leung JM, Lawley TD, Shen A. 2013.
803 Global analysis of the sporulation pathway of Clostridium difficile. PLoS Genet 9.
804

805 **FIGURES**

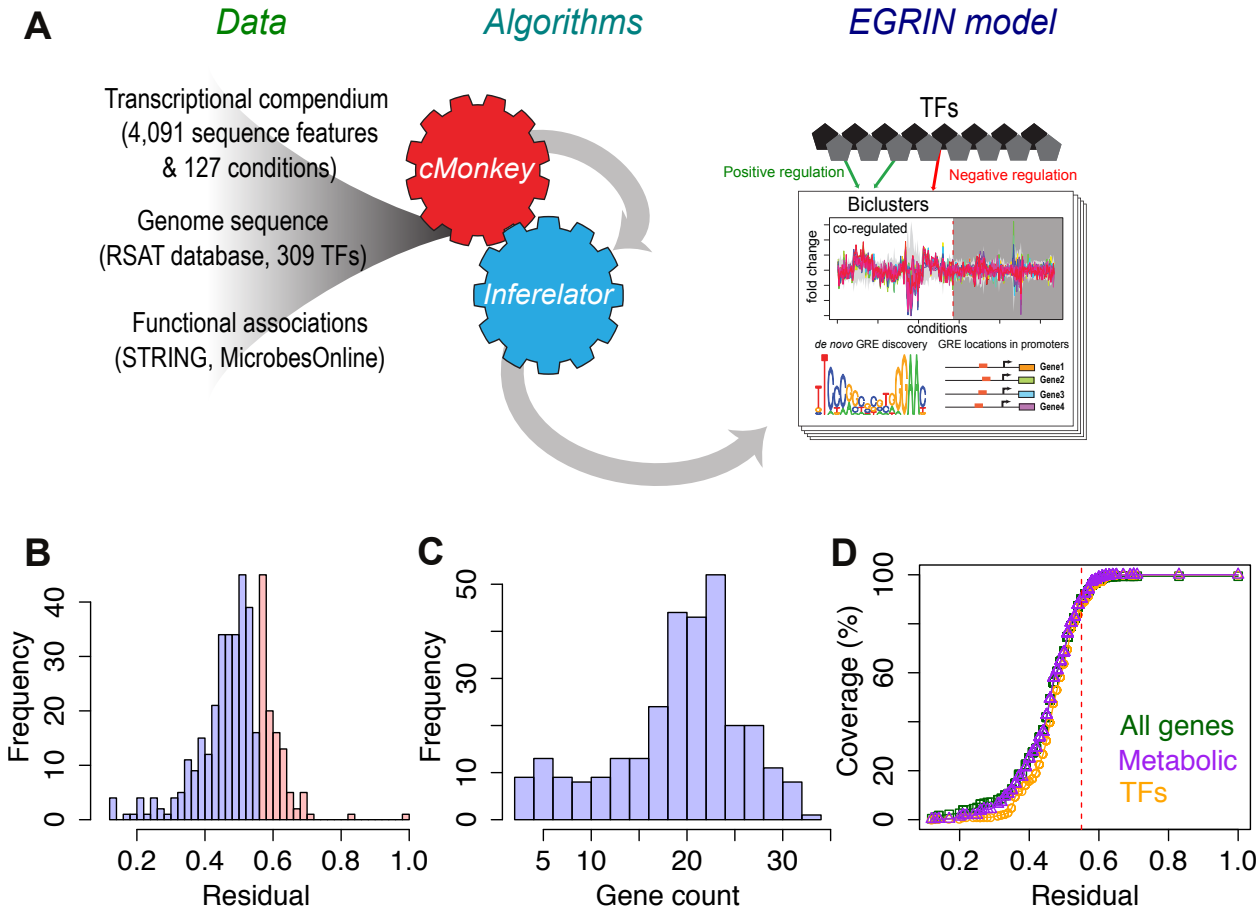

806

807 **Figure 1. Inference pipeline and general properties of the resulting Environment Gene**
808 **Regulatory Influence Network (EGRIN) model of *C. difficile*.** (A) Framework used to build the
809 EGRIN model. (B) Distribution of residual values for the 406 detected co-regulated gene modules.
810 297 gene modules had residual values equal or lower than 0.55 (shown in purple) and were
811 labelled as high quality. (C) Distribution of gene count for the high quality gene modules. (D)
812 Coverage of all genes (4,018), the subset of metabolic genes (1,030) and TFs (309) by EGRIN
813 modules for different residual thresholds. The red dashed line indicates the 0.55 residual cutoff.

814

815

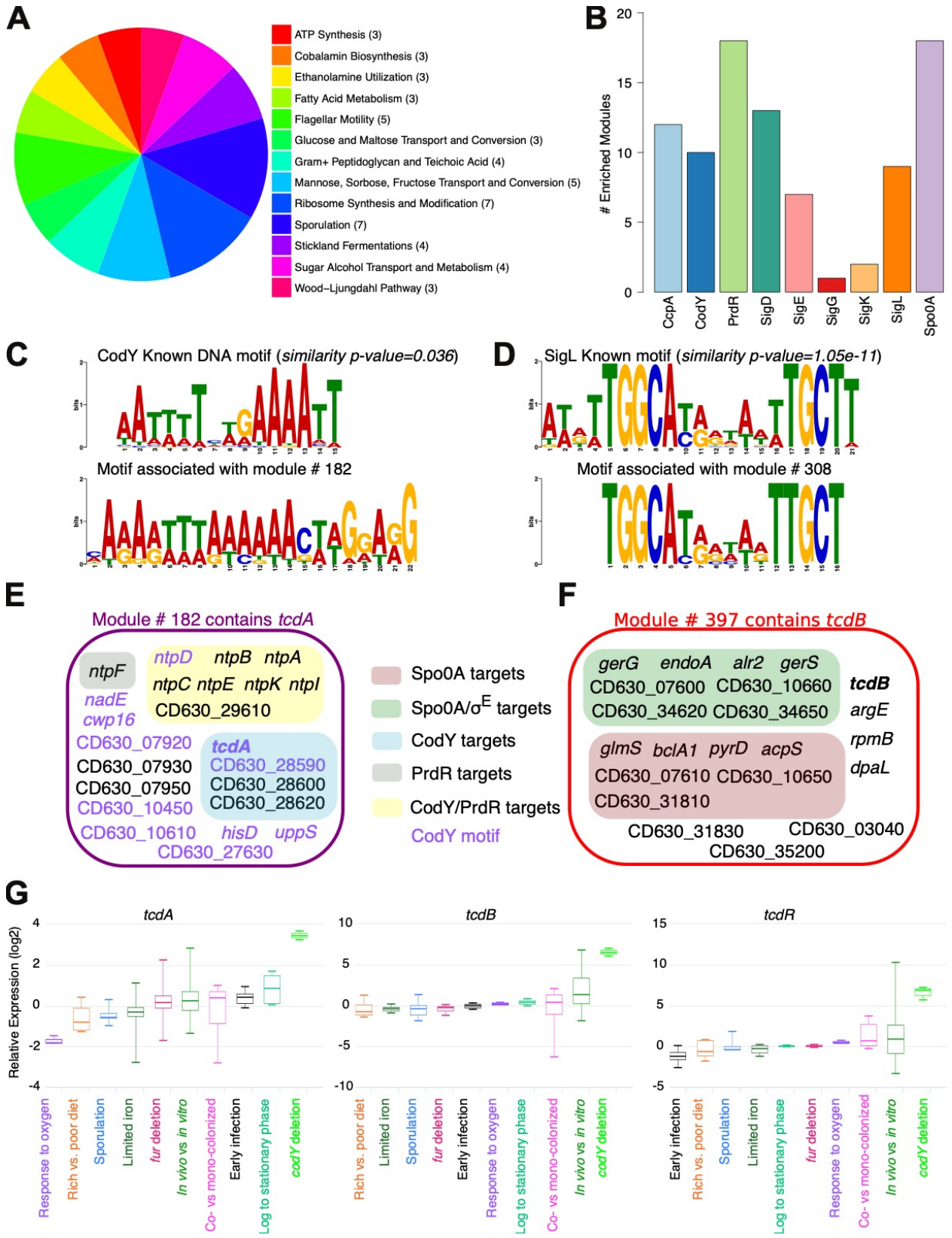
A
ATP Synthesis (3)
Cobalamin Biosynthesis (3)
Ethanolamine Utilization (3)
Fatty Acid Metabolism (3)
Flagellar Motility (5)
Glucose and Maltose Transport and Conversion (3)
Gram+ Peptidoglycan and Teichoic Acid (4)
Mannose, Sorbose, Fructose Transport and Conversion (5)
Ribosome Synthesis and Modification (7)
Sporulation (7)
Stickland Fermentations (4)
Sugar Alcohol Transport and Metabolism (4)
Wood–Ljungdahl Pathway (3)
B
Enriched Modules
CcpA
CodY
PrdR
SigD
SigE
SigG
SigK
SigL
Spo0A
C
CodY Known DNA motif (similarity p-value=0.036)
Motif associated with module # 182
D
SigL Known motif (similarity p-value=1.05e-11)
Motif associated with module # 308
E
Module # 182 contains tcdA
ntpF
nadE
cwp16
ntpD ntpB ntpA
ntpC ntpE ntpK ntpI
CD630_29610
CD630_07920
CD630_07930
CD630_07950
CD630_10450
tcdA
CD630_28590
CD630_28600
CD630_28620
CD630_10610
hisD uppS
CD630_27630
Spo0A targets
Spo0A/σE targets
CodY targets
PrdR targets
CodY/PrdR targets
CodY motif
F
Module # 397 contains tcdB
gerG endoA alr2 gerS
CD630_07600 CD630_10660
CD630_34620 CD630_34650
tcdB
argE
rpmB
dpaL
glmS bclA1 pyrD acpS
CD630_07610 CD630_10650
CD630_31810
CD630_31830
CD630_03040
CD630_35200
G
tcdA
tcdB
tcdR
Relative Expression (log2)
Response to oxygen
Rich vs. poor diet
Sporulation
Limited iron
fur deletion
In vivo vs in vitro
Co- vs mono-colonized
Early infection
Log to stationary phase
codY deletion

817 **Figure 2. The Environment Gene Regulatory Influence Network model of *C. difficile***
818 **recapitulates known biology of the pathogen.** (A) Co-regulated gene modules are enriched
819 with functional terms derived from expert curated annotation of the *C. difficile* genome (22). The
820 pie chart shows terms over-represented in three or more modules. Number of modules associated
821 with each functional term is shown in parenthesis. (B) Enriched gene modules among nine (out
822 of 13) manually-defined and experimentally supported TF regulons (compiled from publicly
823 available data in Table S1). (C) EGRIN identified the known DNA binding motif of CodY (65). (D)
824 EGRIN also identified the known DNA binding motif of SigL (66). Motif comparisons were
825 performed using Tomtom (60). (E) The EGRIN model recapitulated the previously reported
826 influence of CodY on *tcdA* expression. The module #182 contains *tcdA*, it is enriched with
827 members of the CodY regulon and contains a motif (shown in panel C) similar to the
828 experimentally determined CodY motif. (F) The EGRIN model also captured the interaction
829 between toxin expression and sporulation via module #397 that contains *tcdB* and is enriched
830 with genes regulated by sporulation-related transcriptional regulators. **(**G) Expression profiles of
831 *tcdAB* and *tcdR* (positive regulator of the pathogenicity loci). Highest expression of the toxin genes
832 and their activator was observed in the *codY* single deletion condition (light green box).
833

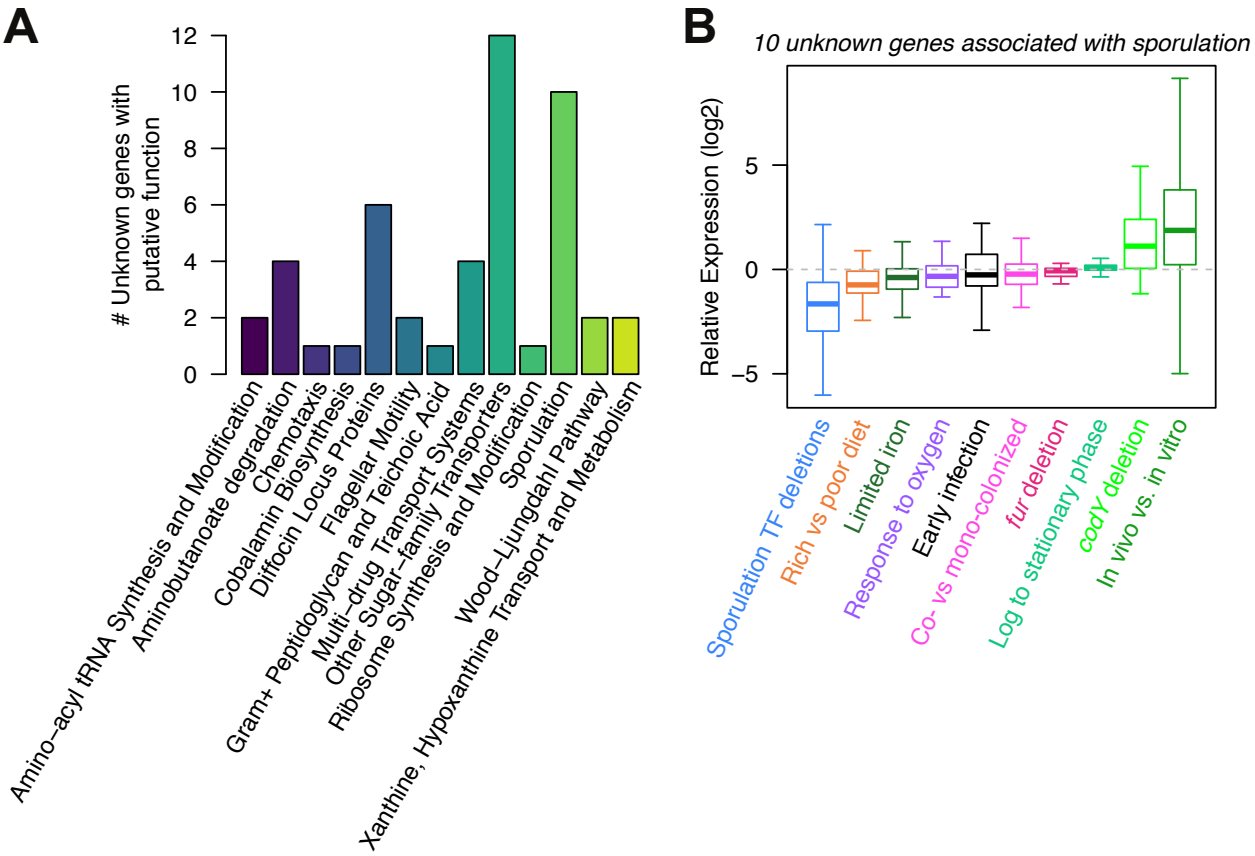

C

Predicted role	Enriched modules	Enriched TF regulons	Uncharacterized genes
Other Sugar-family Transporters	43	NA	CD630_04371, CD630_09341, CD630_12100, CD630_13011, CD630_13781, CD630_13782, CD630_15970, CD630_17720, CD630_20101, CD630_20751, CD630_29661, CD630_31110
Sporulation	206, 251	Spo0A, SigE, SigG	CD630_01310, CD630_02140, CD630_10650, CD630_10660, CD630_19280, CD630_23740, CD630_23750, CD630_24430, CD630_26340, CD630_32590
Diffocin Locus Proteins	136	NA	CD630_12420, CD630_12430, CD630_12440, CD630_13760, CD630_14150, CD630_14160
Aminobutanoate degradation	48	CodY, PrdR	CD630_05100 , CD630_05101, CD630_08760, CD630_08780
Multi-drug transport systems	29	NA	CD630_03790, CD630_03800, CD630_10991, CD630_33681

Figure 3. The EGRIN model offers insights on potential functions of uncharacterized genes of *C. difficile*. Hypotheses regarding the functions of 48 uncharacterized genes were generated based on their membership in high quality co-regulated gene modules significantly enriched with

839 specific functional terms. (A) Barplot with the number of unknown genes associated with each
840 functional term (from the *C. difficile* genome annotation in Girinathan et al. (22)). (B) The
841 involvement of 10 uncharacterized genes in sporulation was supported by the observed strongest
842 and significant down-regulation in single deletion strains of transcriptional regulators of
843 sporulation (*spo0A*, *sigEFGK*, *spoIIID*). (C) Locus tag of uncharacterized genes associated with
844 selected functional terms.
845

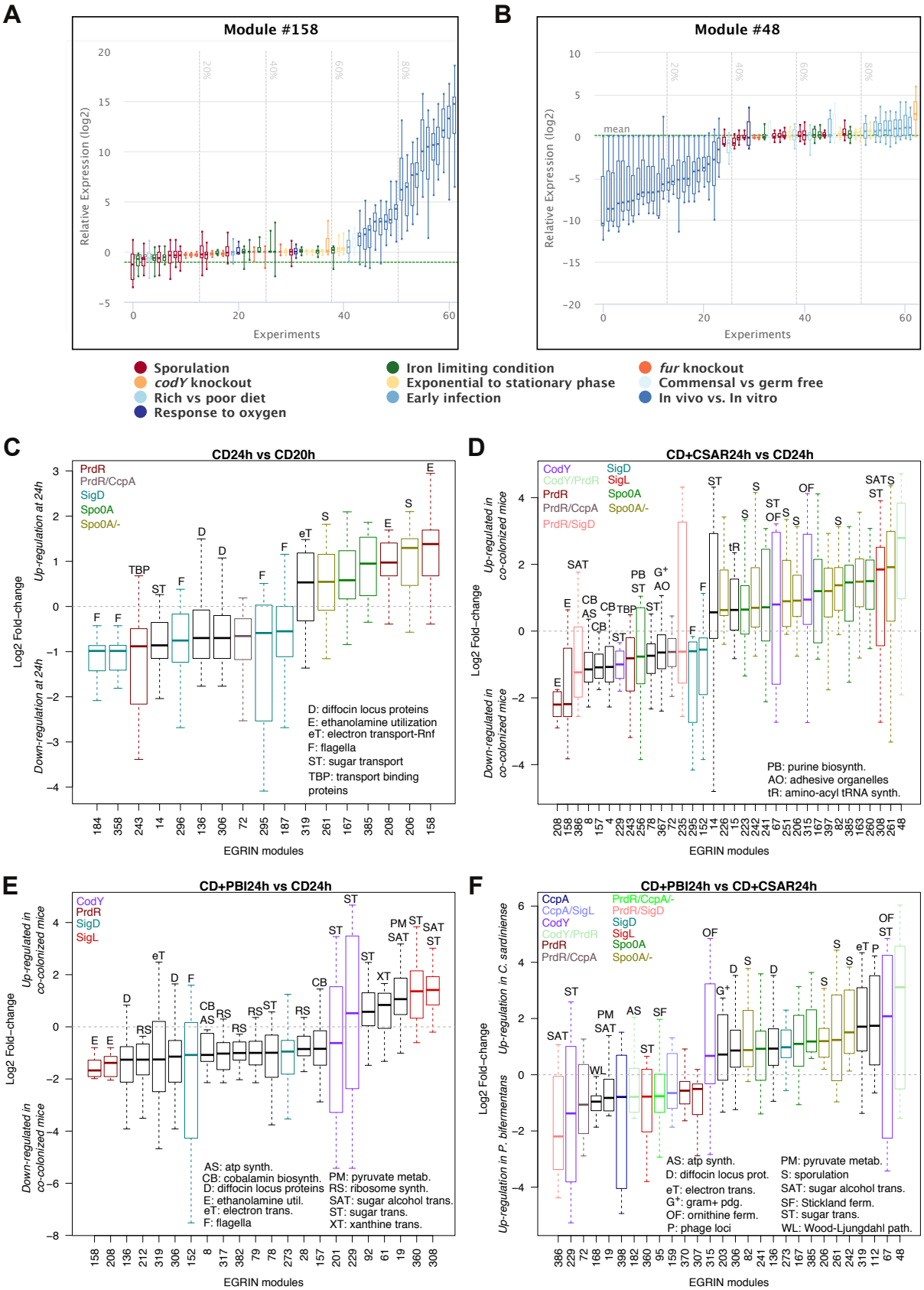
A
Module #158
Relative Expression (log2)
Experiments
B
Module #48
mean
Relative Expression (log2)
Experiments
Sporulation
codY knockout
Rich vs poor diet
Response to oxygen
Iron limiting condition
Exponential to stationary phase
Early infection
fur knockout
Commensal vs germ free
In vivo vs. In vitro
C
CD24h vs CD20h
PrdR
PrdR/CcpA
SigD
Spo0A
Spo0A/-
Log2 Fold-change
Up-regulation at 24h
Down-regulation at 24h
D: diffocin locus proteins
E: ethanolamine utilization
eT: electron transport-Rnf
F: flagella
ST: sugar transport
TBP: transport binding proteins
EGRIN modules
D
CD+CSAR24h vs CD24h
CodY
CodY/PrdR
PrdR
PrdR/CcpA
PrdR/SigD
SigD
SigL
Spo0A
Spo0A/-
Log2 Fold-change
Up-regulated in co-colonized mice
Down-regulated in co-colonized mice
PB: purine biosynth.
AO: adhesive organelles
tR: amino-acyl tRNA synth.
EGRIN modules
E
CD+PBI24h vs CD24h
CodY
PrdR
SigD
SigL
Log2 Fold-change
Up-regulated in co-colonized mice
Down-regulated in co-colonized mice
AS: atp synth.
CB: cobalamin biosynth.
D: diffocin locus proteins
E: ethanolamine util.
eT: electron trans.
F: flagella
PM: pyruvate metab.
RS: ribosome synth.
SAT: sugar alcohol trans.
ST: sugar trans.
XT: xanthine trans.
EGRIN modules
F
CD+PBI24h vs CD+CSAR24h
CcpA
CcpA/SigL
CodY
CodY/PrdR
PrdR
PrdR/CcpA
PrdR/CcpA/-
PrdR/SigD
SigD
SigL
Spo0A
Spo0A/-
Log2 Fold-change
Up-regulation in C. sardiniense
Up-regulation in P. bifermentans
AS: atp synth.
D: diffocin locus prot.
eT: electron trans.
G+: gram+ pdg.
OF: ornithine ferm.
P: phage loci
PM: pyruvate metab.
S: sporulation
SAT: sugar alcohol trans.
SF: Stickland ferm.
ST: sugar trans.
WL: Wood-Ljungdahl path.
EGRIN modules

847 **Figure 4. The EGRIN model identifies TFs driving the *in vivo* response of *C. difficile* when**
848 **interacting with gut commensals *P. bifermentans* (PBI) and *C. sardiniense* (CSAR).** (A)
849 Expression profile of module #158. (B) Expression profile of module #48. (C) EGRIN modules
850 enriched with genes differentially expressed (absolute log2 fold-change > 1 and adjusted p-value
851 < 0.05) in *C. difficile* mono-colonized mice at 24 vs 20 hours of infection. X-axis shows module
852 IDs. Modules were annotated according to their functional enrichment and overlap with manually
853 curated TF regulons (Table S1). (D) Enriched EGRIN modules in *C. sardiniense*+*C. difficile* co-
854 colonized mice vs *C. difficile* mono-colonized mice at 24 hours of infection. Due to space
855 constraint, only abbreviations of functional terms not shown in other panels are displayed. (E)
856 Enriched EGRIN modules in *P. bifermentans*+*C. difficile* co-colonized mice vs *C. difficile* mono-
857 colonized mice at 24 hours of infection. (F) Enriched EGRIN modules in *P. bifermentans*+*C.*
858 *difficile* co-colonized mice vs *C. sardiniense*+*C. difficile* co-colonized mice at 24 hours of infection.
859 For all comparisons, only modules with absolute median fold-changes > 0.5, and enriched with
860 TF regulons or functional categories are displayed.
861
862
863

A

icdf834 constraints-based metabolic model of *C. difficile*	
Genes	834
Reactions	1227
Metabolites	807

B

In vivo constraints-based metabolic model of *C. difficile*	
Genes	834 (838)
Reactions	665 (673)
Metabolites	594 (601)

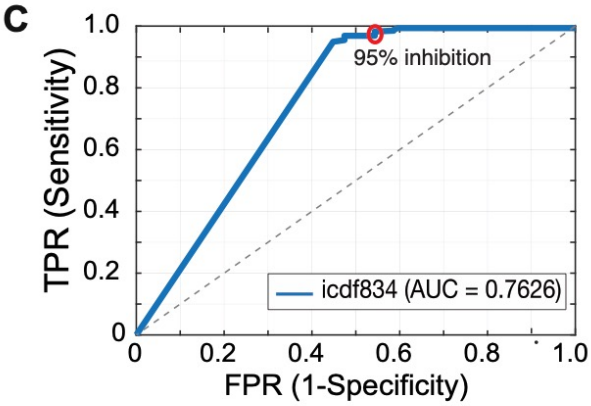

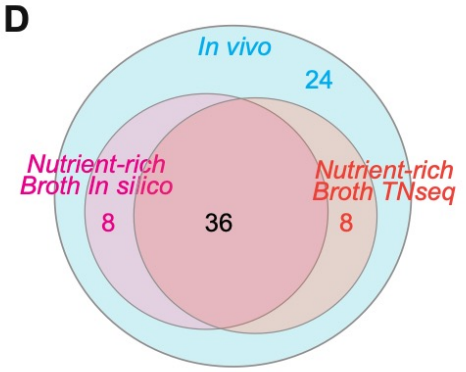

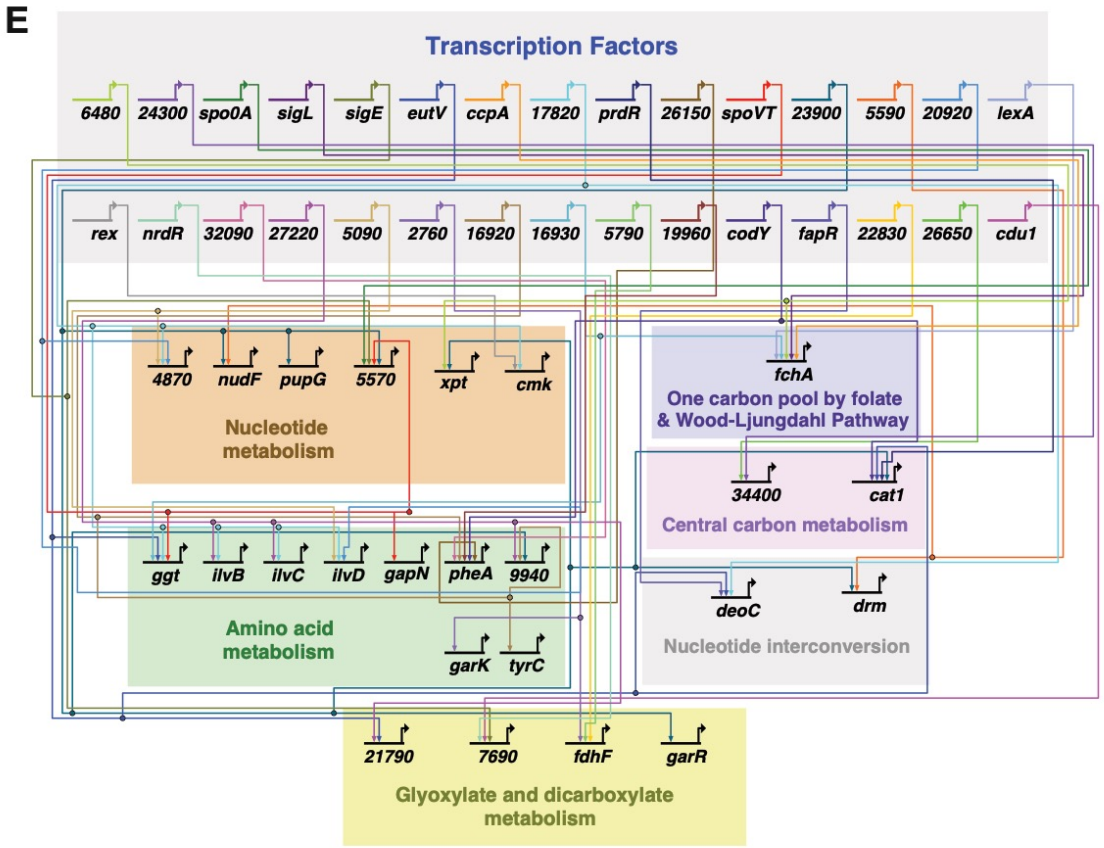

Figure 5. Metabolic model predictions. (A) Details of the *in vitro* metabolic model of *C. difficile* 630 (41). (B) Details of icdf838 metabolic model of *C. difficile* 630. Initial *in vivo* model was derived

867 using the GIMME algorithm (46) where only the active reactions are included from *in vivo*
868 transcriptome. The numbers in parentheses indicate the number of genes, reactions and
869 metabolites in the icdf838 model after adding the required *in vivo* exchanges and transports. (C)
870 ROC curve showing the accuracy of icdf834-predicted gene essentiality in nutrient rich medium
871 evaluated against a Tn-seq functional screen (35). Red circle indicates the 95% growth inhibition
872 as threshold. (D) Venn diagram showing the number of model-predicted essential genes for
873 growth of *C. difficile 630 in vitro* vs *in vivo*. (E) BioTapestry visualization of *in vivo* gene regulatory
874 network for *C. difficile* 630: All 24 *in vivo*-specific essential genes that are regulated by
875 transcription factors (TFs) are shown. Transcriptional regulators are derived from EGRIN. The
876 network includes all TFs that regulate more than four *in vivo* essential genes. The genes and TFs
877 shown as five digit numbers represent the nomenclature preceded by 'CD630_' (e.g. 27220
878 indicates CD630_27220).
879
880

A

Module 182

Residual	Gene Count	Condition Count
0.56	24	65

Bicluster expression profile

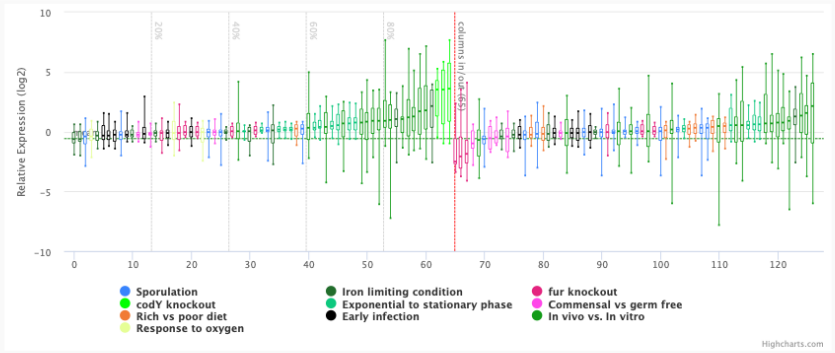

de novo identified motifs are listed below

Motif 1	Motif 1 e-value		Motif 2	Motif 2 e-value	
CAAAATTTAAAAAACTAGGAGG	0.000000000023	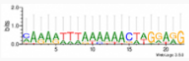	GAAAGGTGATT	0.06	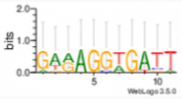

B

This module is predicted to be regulated by the following regulators

TF Influences (Hypergeometric)

CD630_12750 - codY — Type: Gene

Product: Transcriptional regulator, GTP-sensing pleiotropic repressor | **Pathway:** | **COG:** Transcription

CD630_32450 - prdR — Type: Gene

Product: Transcriptional regulator, sigma-54-dependent | **Pathway:** | **COG:** Transcription

TF Influences (Inferelator)

CD630_11770 - fapR — Type: Gene

Product: Tracriptional regulator, DeoR family (Fatty acid and phospholipid biosynthesis regulator) | **Pathway:** | **COG:** Transcription

CD630_20480 - — Type: Gene

Product: Transcriptional regulator, RpiR family | **Pathway:** | **COG:** Transcription

CD630_26420 - sigG — Type: Gene

Product: RNA polymerase sigma-G factor | **Pathway:** | **COG:** Transcription

The module is significantly enriched with genes associated to the indicated functional terms

Enriched Functional Terms	Number:
ATP_Synthesis	3.5.9

C

Genes that are included in this module

Displaying 1 - 24 of 24

Title	Short Name	Product	Alt Names	Function	Essentiality *
CD630_06630	*tcdA*	Toxin A	Toxin A (EC 2.4.1.-)		
CD630_07920		Putative membrane protein, DUF81 family	Probable membrane transporter protein		
CD630_07930		Putative membrane protein, DUF81 family	Probable membrane transporter protein		
CD630_07940	*nadE*	NH3-dependent NAD(+) synthetase	NH(3)-dependent NAD(+) synthetase (EC 6.3.1.5)	Catalyzes the ATP-dependent amidation of deamido-NAD to form NAD. Uses ammonia as a nitrogen source.	Yes

881

882 **Figure 6. An example module page of the *C. difficile* Portal.** Module #182, associated with
883 CodY and shown in Fig 2D is used as an example. (A) Each module page includes general
884 statistics of the module (residual score, gene count), displays the module expression profile in the
885 compiled transcriptional compendium and the detected motifs. (B) A module page also offers
886 information about the potential transcriptional regulators of the module. Putative regulators are
887 defined based on over-representation of manually compiled TF regulons (assessed using
888 hypergeometric test) and based on the Inferelator predictions. (C) Each module page includes a
889 list of its gene members with a brief description of each gene. This information includes gene
890 name, product, alternative names, function and essentiality. In the example, only the first four
891 genes (out of 24) are shown. The user can click in any gene to visit the corresponding gene page.
892
893

894 # TABLES

895 **Table 1. Datasets used for generating *C. difficile* transcriptional compendium**

Condition	GEO Series Accession	# Transcriptomes[a]	# Controls[b]
Early infections (0h, 30 mins, 60 mins, 120 mins)	GSE18407	12	NA[c]
In vivo vs *in vitro* (8h, 14h, 38h)	GSE43305	32	NA[c]
Iron limitation	GSE109453 GSE120189	15	15[d]
fur deletion	GSE69218 GSE120189	12	12[d]
Response to oxygen	GSE109175	3	3
Response to commensals and diet	GSE60751	8	8[e]
Rich diet vs Poor diet	GSE60751	8	8[e]
Transition from exponential to stationary phase	GSE115054	16	NA[c]
codY KO	GSE23192	3	NA[c]
Sporulation (*spo0A* KO, *sigEFGK* KOs, *spoIIID* KO)	GSE45977 GSE63777	18	6

896 [a]Refers to the number of arrays used as numerator when estimating log2 ratios
897 [b]Control arrays were averaged and used as denominator when estimating log2 ratios
898 [c]Not Applicable. Dual channel array and therefore the control was included in each array
899 [d]Six samples used as controls were also considered as main transcriptome in other comparisons
900 [e]Samples used as controls were also considered as main transcriptome in other comparisons

901 **SUPPLEMENTARY FIGURES**

902

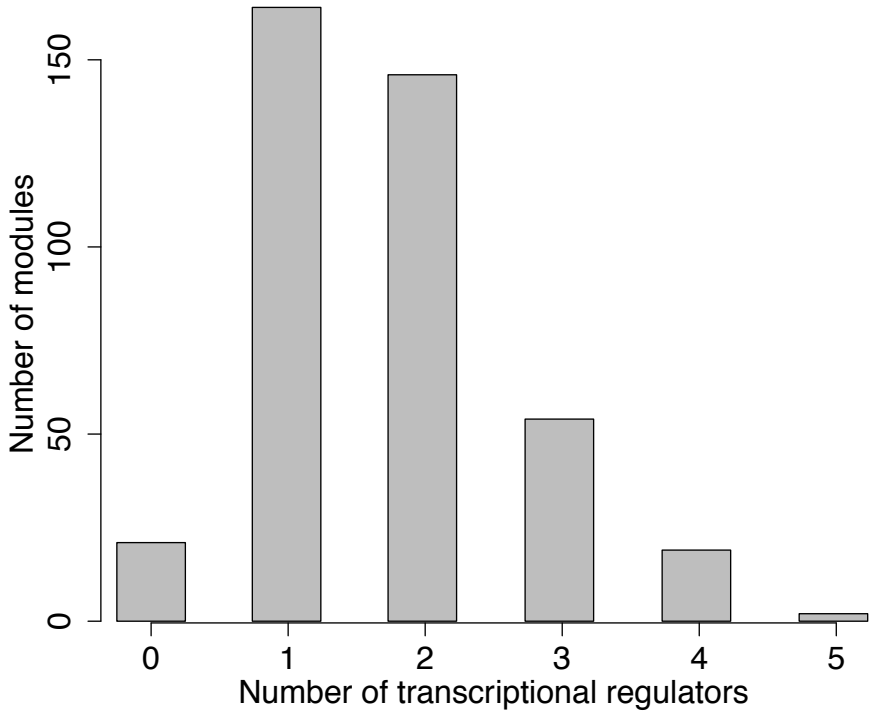

903

904 **Figure S1. Number of Inferelator-predicted transcriptional regulators of modules in the**

905 **EGRIN model.**

906

907

908

A

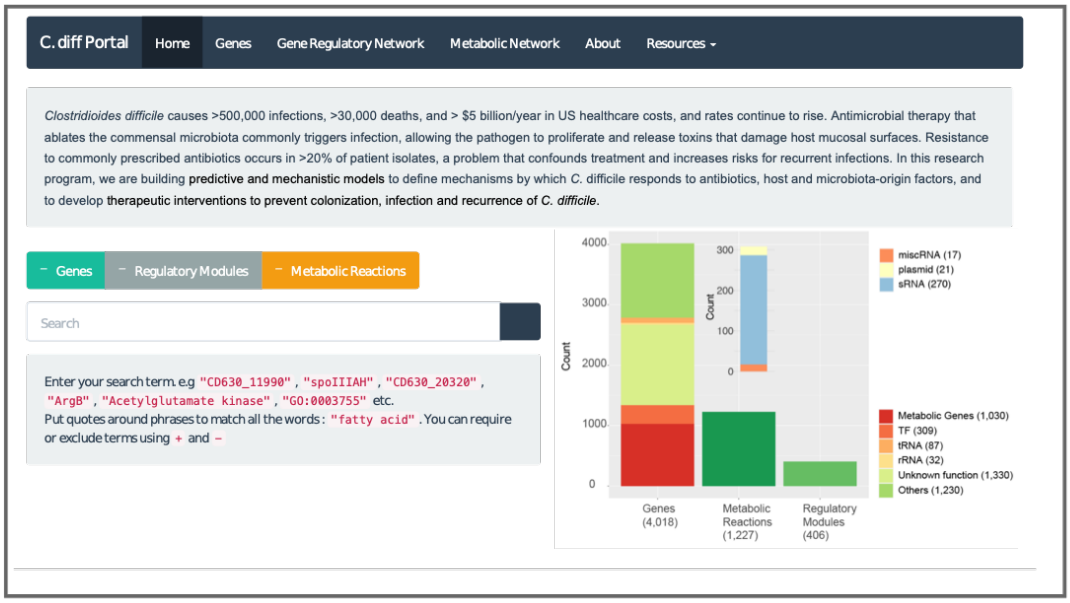
C. diff Portal
Home
Genes
Gene Regulatory Network
Metabolic Network
About
Resources
Clostridioides difficile causes >500,000 infections, >30,000 deaths, and > $5 billion/year in US healthcare costs, and rates continue to rise. Antimicrobial therapy that ablates the commensal microbiota commonly triggers infection, allowing the pathogen to proliferate and release toxins that damage host mucosal surfaces. Resistance to commonly prescribed antibiotics occurs in >20% of patient isolates, a problem that confounds treatment and increases risks for recurrent infections. In this research program, we are building predictive and mechanistic models to define mechanisms by which C. difficile responds to antibiotics, host and microbiota-origin factors, and to develop therapeutic interventions to prevent colonization, infection and recurrence of C. difficile.
Genes
Regulatory Modules
Metabolic Reactions
Search
Enter your search term. e.g "CD630_11990", "spoIIIAH", "CD630_20320", "ArgB", "Acetylglutamate kinase", "GO:0003755" etc.
Put quotes around phrases to match all the words: "fatty acid". You can require or exclude terms using + and −
Count
Genes (4,018)
Metabolic Reactions (1,227)
Regulatory Modules (406)
miscRNA (17)
plasmid (21)
sRNA (270)
Metabolic Genes (1,030)
TF (309)
tRNA (87)
rRNA (32)
Unknown function (1,330)
Others (1,230)

B

CD630_06630 tcdA
Title
Product
Short Name
Synonyms
Start
End
Strand
Sequence Name
Essentiality
CD630_06630
Toxin A
tcdA
795843
803975
+
Chromosome
Additional annotations
Expression profile of the gene across conditions
Relative Expression (log2)
Sporulation
codY knockout
Rich vs poor diet
Response to oxygen
Iron limiting condition
Exponential to stationary phase
Early infection
fur knockout
Commensal vs germ free
In vivo vs. In vitro
Highcharts.com
CD630_06630 tcdA is a member of the following modules
Module
Expression Plot
Gene Count
Motif 1 e-value
Motif 1 logo
Motif 2 e-value
Motif 2 logo
Residual
182
24
0.000000000023
0.06
0.56
264
21
1.9e-16
0.71

909

910 **Figure S2. The Cdiff Web Portal.** (A) Home page of the Cdiff Portal. Users can explore the
911 gene regulatory network model and the metabolic model for *C. difficile*. In addition, all files are
912 accessible in the resource tab. The search bar facilitates website exploration. (B) An example
913 gene page of the *C. difficile* Portal.
914
915

916 # SUPPLEMENTARY TABLES

917

918 **Table S1. Compiled TF regulons**

Regulator	Regulon Size	Supporting Data	Reference
CcpA	194[a]	Protein-DNA binding, transcriptomics, *in silico*[b]	(3, 67)
CodY	160[c]	Protein-DNA binding, transcriptomics	(65)
Fur	19	Transcriptomics, *in silico*[b]	(68, 69)
PrdR	181	Transcriptomics	(24)
SigB	57	Transcriptomics	(15)
SigD	159	Transcriptomics	(70)
SigE	96	Transcriptomics	(30)
SigF	25		
SigG	46		
SigH	40	Transcriptomics, *in silico*[b]	(4)
SigK	54	Transcriptomics	(30)
SigL	46[d]	Transcriptomics, *in silico*[b]	(66)
Spo0A	276[e]	Transcriptomics	(71)

919 [a]Only genes classified as CcpA-dependent (in the presence or absence of glucose) by Antunes
920 et al. 2012 (3) were included
921 [b]*In silico* search of the binding motif of the corresponding regulator within the genes and their
922 promoter sequences
923 [c]Only genes negatively influenced by CodY were included
924 [d]Only genes with SigL motif and down-regulated in *sigL* deletion were included
925 [e]Only genes positively influenced by Spo0A were included

926

927

928 **Table S2. General properties of modules associated with the pathogenicity loci**

Gene	Locus tag	Module[a]	Residual	Functional enrichment[b]	Enriched TF regulons[b]	Inferelator predicted regulators[b]
tcdR	CD_06590	31	0.46	NF	NF	SigG, SpoVT
		336	0.54	NF	NF	FapR, CD_16930
tcdB	CD_06600	284	0.63	NF	NF	CD_06930, CD_17820
		397	0.49	NF	Spo0A, SigE	SpoVT, CD_06290
tcdE	CD_06610	31	0.46	NF	NF	SigG, SpoVT
		138	0.61	NF	NF	CD_06290, CD_12390, SpoVT
tcdA	CD_06630	182	0.56	ATP synthesis	CodY, PrdR	FapR, CD_20480, SigG
		264	0.71	NF	NF	SigV
tcdC	CD_06640	146	0.52	NF	NF	CD_27320, PhoU
		395	0.51	NF	NF	CD_18100, CD_35440

929 [a]Modules that contain the corresponding member of the pathogenicity loci
930 [b]Refers to the information shown for the corresponding module on the Cdiff Web Portal
931

932 **Table S3. Model predicted essential genes *in vivo***

Locus tag	Gene name	Gene product/function	Pathway	In silico predictions		Expt
				Essentiality in vivo	Essentiality nutrient-rich in vitro	Essentiality Nutrient-rich in vitro (Tn-seq)
CD630_09940	G12WB-1109	serine-pyruvate aminotransferase	Alanine, aspartate and glutamate metabolism	Essential	Non-Essential	Non-Essential
CD630_05800	gapN	glyceraldehyde-3-phosphate dehydrogenase	Valine, leucine and isoleucine metabolism	Essential	Non-Essential	Non-Essential
CD630_15340	ggt	gamma-glutamyltranspeptidase	Alanine, aspartate and glutamate metabolism	Essential	Non-Essential	Non-Essential
CD630_23430	cat1	succinyl-CoA:coenzyme A transferase	Butanoate fermentation; Methionine Biosynthesis	Essential	Non-Essential	Non-Essential
CD630_34400	G12WB-3619	glycoside hydrolase-type carbohydrate-binding protein	Glycolysis	Essential	Non-Essential	Non-Essential
CD630_30840	garK	glycerate kinase	Glycine, serine and threonine metabolism	Essential	Non-Essential	Non-Essential
CD630_28130	garR	tartronate semialdehyde reductase	Glyoxylate and dicarboxylate metabolism	Essential	Non-Essential	Non-Essential
CD630_33170	fdhF	formate dehydrogenase-H	Glyoxylate and dicarboxylate metabolism	Essential	Non-Essential	Non-Essential
CD630_21790	G12WB-2336	anaerobic dehydrogenase	Glyoxylate and dicarboxylate metabolism	Essential	Non-Essential	Non-Essential
CD630_07690	G12WB-880	oxidoreductase subunit	Glyoxylate and dicarboxylate metabolism	Essential	Non-Essential	Non-Essential

CD630_12240	pupG	purine nucleoside phosphorylase	Purine metabolism	Essential	Non-Essential	Non-Essential
CD630_07190	fchA	methenyltetrahydrofolate cyclohydrolase	One carbon pool by folate; Wood-Ljungdahl pathway	Essential	Non-Essential	Non-Essential
CD630_15660	ilvB	acetolactate synthase large subunit	Valine, leucine and isoleucine metabolism	Essential	Non-Essential	Non-Essential
CD630_12230	drm	phosphopentomutase	Nucleotide interconversion	Essential	Non-Essential	Non-Essential
CD630_20140	ilvD	dihydroxy-acid dehydratase	Valine, leucine and isoleucine metabolism	Essential	Non-Essential	Non-Essential
CD630_15020	deoC	deoxyribose-phosphate aldolase	Nucleotide interconversion	Essential	Non-Essential	Non-Essential
CD630_18390	tyrC	prephenate dehydrogenase	Phenylalanine, tyrosine and tryptophan biosynthesis	Essential	Non-Essential	Non-Essential
CD630_18360	pheA	bifunctional chorismate mutase/prephenate dehydratase	Phenylalanine, tyrosine and tryptophan biosynthesis	Essential	Non-Essential	Non-Essential
CD630_12200	nudF	NUDIX family hydrolase	Purine metabolism	Essential	Non-Essential	Non-Essential
CD630_23300	xpt	xanthine phosphoribosyltransferase	Purine metabolism	Essential	Non-Essential	Non-Essential
CD630_05570	G12WB-669	uridine kinase	Pyrimidine metabolism	Essential	Non-Essential	Non-Essential
CD630_04870	G12WB-599	carbon-nitrogen hydrolase	Pyrimidine metabolism	Essential	Non-Essential	Non-Essential
CD630_18160	cmk	cytidylate kinase	Pyrimidine metabolism	Essential	Non-Essential	Non-Essential

CD630_15650	ilvC	ketol-acid reductoisomerase	Valine, leucine and isoleucine metabolism	Essential	Non-Essential	Non-Essential